Marine Biodiversity (2021) 51:54
https://doi.org/10.1007/s12526-021-01188-7

SENCKENBERG

ORIGINAL PAPER

New Paracalanidae species from the central coast of Brazil: morphological description and molecular evidence

Flavia Guerra Vieira-Menezes[1] · Cristina de Oliveira Dias[1,2] · Astrid Cornils[3] · Rosane Silva[4] · Sérgio Luiz Costa Bonecker[1]

Received: 5 February 2020 / Revised: 30 March 2021 / Accepted: 3 April 2021

Abstract

Two new species of Paracalanidae, Giesbrecht, 1893, have been described. *Paracalanus brasiliensis* sp. nov. and *Bestiolina brasiliensis* sp. nov. were registered in four estuaries on the central coast of Brazil. *Paracalanus brasiliensis* sp. nov. females differ from their congeners mainly with regard to body size, the structure of swimming legs 1–4, absence of bristles in the coxopodites, spinules between the spines in the third segment of the exopodite, and the shape of the seminal receptacles. The uniformity of the number of spinules and their location on the anterior face of the second exopodite of legs 2–3 and the absence of spinules on the endopodite of legs 3–4 differentiate *Bestiolina brasiliensis* sp. nov. females from other *Bestiolina* Andronov, 1991, species. In the males of both species, the main diagnostic features (swimming leg seta, spine formula, and ornamentation) are generally observed in females with a few additional characteristics. Genetic divergence analyses based on partial mitochondrial COI (mtCOI) sequences revealed no genetic divergence between *Paracalanus brasiliensis* sp. nov. and *Paracalanus* sp. E. sensu Cornils and Held (2014), demonstrating that they are mutually conspecific. mtCOI sequence data from *Bestiolina brasiliensis* sp. nov. identified a clade with high bootstrap support that separated the specimens in this study from other *Bestiolina* species. The present report provides the first morphological description of females and males of both *Paracalanus brasiliensis* sp. nov. and *Bestiolina brasiliensis* sp. nov. and presents molecular evidence for species specificity. Matters regarding the validity of these species are also discussed.

Keywords *Paracalanus brasiliensis* sp. nov. · *Bestiolina brasiliensis* sp. nov. · Estuary · mtCOI gene

This article is registered in ZooBank under http://zoobank.org/E80A6743-B925-48AA-84A6-4CBDA7987C51

Communicated by S. Ohtsuka

✉ Cristina de Oliveira Dias
crcldias@hotmail.com

[1] Instituto de Biologia, Departamento de Zoologia, Universidade Federal do Rio de Janeiro, Av. Carlos Chagas Filho, 373, CCS, Bloco A, Sala A0-084, Ilha do Fundão, Rio de Janeiro 21.941-902, RJ, Brazil

[2] Programa de Engenharia Ambiental-PEA, Escola Politécnica, Centro de Tecnologia, Universidade Federal do Rio de Janeiro, Avenida Athos da Silveira Ramos, 149, Bl. A, 2° andar, Sala DAPG, Ilha do Fundão, Rio de Janeiro, RJ 21941-909, Brazil

[3] Alfred-Wegener-Institut, Helmholtz-Zentrumfür Polar- und Meeresforschung, Am AltenHafen 26, 27568 Bremerhaven, Germany

[4] Instituto de Biofísica Carlos Chagas Filho, Departamento de Biofísica, Universidade Federal do Rio de Janeiro, Av. Carlos Chagas Filho, 373, CCS, Bloco G, Sala G1-019, Ilha do Fundão, Rio de Janeiro, RJ 21941-902, Brazil

Published online: 31 May 2021

Introduction

Many planktonic marine crustaceans, such as copepods, have cosmopolitan distributions (Boxshall and Defaye 2008). Increasing evidence of cryptic speciation has emphasized the need to re-evaluate the status of copepod species complexes via molecular and morphological studies to obtain a clearer picture of the distributions of these pelagic marine organisms and their evolutionary history (Cornils and Held 2014; Bode et al. 2017). Copepod species identification is often based on body tagma, segmentation, and the armor of cephalic and thoracic appendages (Huys and Boxshall 1991). These characteristics are generally only developed in adult organisms, and thus, the identification of individuals in various juvenile life stages (nauplii and copepodites) is often impossible (McManus and Katz 2009). Furthermore, copepod identification is challenging because of incomplete or inconsistent taxonomic keys (Bucklin et al. 1996; Goetze 2003; Laakmann et al. 2013).

The Paracalanidae copepod family comprises the genera *Acrocalanus* Giesbrecht, 1888; *Bestiolina* (Andronov, 1991); *Calocalanus* Giesbrecht, 1888; *Delius* (Andronov, 1972); *Mecynocera* Thompson I.C., 1888; *Paracalanus* Boeck, 1865; and *Parvocalanus* Andronov, 1970 (Bradford-Grieve et al. 1999; Bradford-Grieve 2008). The first phylogenetic study of this family confirmed the existence of two species complexes within the *Paracalanus* genus (Cornils and Blanco-Bercial 2013) that were originally established by Sewell (1929): *Paracalanus aculeatus* and *Paracalanus parvus* complexes. This molecular phylogenetic study suggested that the *P. aculeatus* and *P. parvus* complexes had very different phylogenetic affinities within the Paracalanidae family (Cornils and Blanco-Bercial 2013). Specimens of the *P. parvus* species complex may be distinguished from individuals of the *P. aculeatus* complex by differences in antenna segmentation and length, spermatheca shape, and internal bristle length of the caudal branches (Cornils and Blanco-Bercial 2013; Cornils and Held 2014).

Currently, the *P. parvus* species complex comprises seven species: *Paracalanus parvus* (Claus, 1863); *Paracalanus indicus* Wolfenden, 1905; *Paracalanus quasimodo* Bowman, 1971; *Paracalanus nanus* Sars G.O., 1925; *Paracalanus intermedius* Shen & Bai, 1956; *Paracalanus tropicus* Andronov, 1977; and *Paracalanus serrulus* Shen & Lee, 1963 (Walter and Boxshall 2021). Nonetheless, the inclusion of *P. serrulus* and *P. intermedius* in this complex remains questionable (Cornils and Held 2014). In many marine coastal areas, species of the *P. parvus* complex have dominated the planktonic copepod communities present (Di Mauro et al. 2009; Hidaka et al. 2016; Kasapidis et al. 2018; Oda et al. 2018), including those found in Brazilian waters (Sterza and Fernandes 2006; Dias and Bonecker 2008; Araujo 2016; da Rosa et al. 2016; Araujo et al. 2017a, b).

Descriptions of the species within the *P. parvus* species complex have mainly emphasized ornamentation differences on swimming leg surfaces and serration on the outer edges of the exopods (Claus 1863; Bowman 1971; Bradford 1978; Cornils and Held 2014). However, it has been recently shown that some of these morphological characteristics may be insufficient to discriminate between species of the *P. parvus* complex (Kasapidis et al. 2018). The study on the genetic structure of the *P. parvus* complex based on mitochondrial marker genes (cytochrome oxidase c subunit I, COI) has provided evidence of cryptic or pseudo-cryptic speciation and indicated that *Paracalanus parvus* s.s. is not panmictic but geographically restricted to the northern and southeastern Atlantic (Cornils and Held 2014). In addition, a divergent lineage of *Paracalanus parvus* s.l. was detected in the southwestern Atlantic Ocean (*Paracalanus* sp. E).

The *Bestiolina* genus was originally defined to accommodate *Acrocalanus inermis* Sewell, 1912, which differed greatly from all other *Acrocalanus* species (Andronov 1972; Andronov 1991). To date, nine *Bestiolina* species have been described: *Bestiolina inermis* (Sewell, 1912); *Bestiolina similis* (Sewell, 1914); *Bestiolina sinica* (Shen & Lee, 1966); *Bestiolina zeylonica* (Andronov, 1972); *Bestiolina amoyensis* (Li & Huang, 1984); *Bestiolina arabica* Ali, Al-Yaman & Prusova, 2007; *Bestiolina coreana* Moon, Lee & Soh, 2010; *Bestiolina mexicana* Suárez-Morales & Almeyda-Artigas, 2016; and *Bestiolina sarae* Dorado-Roncancio & Gaviria, 2019.

Bestiolina species are concentrated in the coastal tropical regions of the Indo-Pacific, South African Atlantic, Colombian Pacific, and Gulf of Mexico (Moon et al. 2010; Razouls et al. 2005–2021; Dorado-Roncancio et al. 2019). However, it has been speculated that *Bestiolina* species originated from the Indo-Malayan region (Ali et al. 2007). According to Dorado-Roncancio et al. (2019), a poor understanding of the diversity and distributional patterns of the *Bestiolina* genus may be explained by inappropriate sampling techniques (nets with mesh size >200 μm), the small size of the individuals (670–1,008 μm), and confusion regarding the copepodite stages of other paracalanid species.

During a research project that focused on the composition, biomass, and distribution of the zooplankton community of the central Brazilian coast (Araujo et al. 2017a, b), samples were collected from four different estuarine areas (Macaé, São João, Perequê-Açu, and Bracuí). The authors recorded the abundance of the Paracalanidae family with regard to *B. similis*, *P. quasimodo*, *Parvocalanus crassirostris* (Dahl, 1894), and *Paracalanus* spp. (consisting of unidentified specimens and copepodites). Although *Paracalanus* and *Bestiolina* species were present in several samples, individuals could not be assigned to any known species due to observed morphological characteristics that differed from previously described genera.

Because of the scarcity of information regarding both the molecular and taxonomic definitions of Brazilian Paracalanidae, we aimed to present the first morphological description and molecular barcodes (mitochondrial COI) of the new species *Paracalanus brasiliensis* sp. nov. and *Bestiolina brasiliensis* sp. nov. We also compared the molecular results of Brazilian *P. parvus* s.l. specimens with the findings of Cornils and Held (2014).

Material and methods

Surveys were carried out in four estuaries located in Rio de Janeiro state: Macaé (22° 22′ 28″ S and 41° 46′ 30″ W), São João (22° 35′ 54″ S and 41° 59′ 32″ W), Bracuí (22° 57′ 12″ S and 44° 24′ 05″ W), and Perequê-Açu (23° 13′ 01″ S and 44° 42′ 40″ W). Surveys were conducted every 2 months from March 2013 to March 2015 (Fig. 1). In August 2013, logistical problems prevented sampling in the Perequê-Açu estuary, and an additional survey was conducted in this estuary in November 2014.

Zooplankton sampling was performed by horizontal surface tows using cylindrical-conical plankton nets (0.6 m mouth diameter; 200 μm mesh) fitted with a flowmeter (General Oceanics Inc., Miami, FL, USA) that was attached to the net mouth to calculate the volume of water filtered. Each net tow was only conducted for 5 min due to the high density of suspended material in the estuaries. Immediately after collection, the organisms were preserved in 4% buffered formalin for morphological analysis. Another haul was made under the same conditions, and the material obtained was immediately preserved in 99.5% hydrated ethyl alcohol. After 24 h, the alcohol was replaced to maintain DNA integrity in the samples for molecular analysis. Temperature and salinity were measured *in situ* using an HQ40D portable multiparameter probe (Hach Company, Loveland, CO, USA).

Specimens of potentially novel species were sorted, dissected, and identified to a specific level under a Stemi SV6 stereomicroscope (Carl Zeiss, Oberkochen, Germany) and an SZX-ILLB2-100 stereomicroscope (Olympus, Tokyo, Japan). All specimens were preserved in ethanol and deposited in the National Museum (MN) and in the Laboratório Integrado de Zooplâncton e Ictioplâncton (LIZI) of the Universidade Federal do Rio de Janeiro (DZUFRJ Copepoda), Rio de Janeiro, Brazil.

Specimen illustrations and details of the morphological structures used for identification were elaborated in ink from the observations of the structures of specimens dissected under an optical microscope, an Axio Imager 2 differential interferential phase contrast (DIC) microscope (Carl Zeiss), a JSM 5310 scanning electron microscope (SEM, Jeol USA Inc., Peabody, MA, USA), and a Quanta 250 SEM (FEI Company, Hillsboro, OR, USA). Schematic drawings were diagrammed using Adobe Photoshop CS6 (Adobe System Incorporated, San Jose, CA, USA). The body sizes of individuals were measured from the head to the tip of the caudal rami

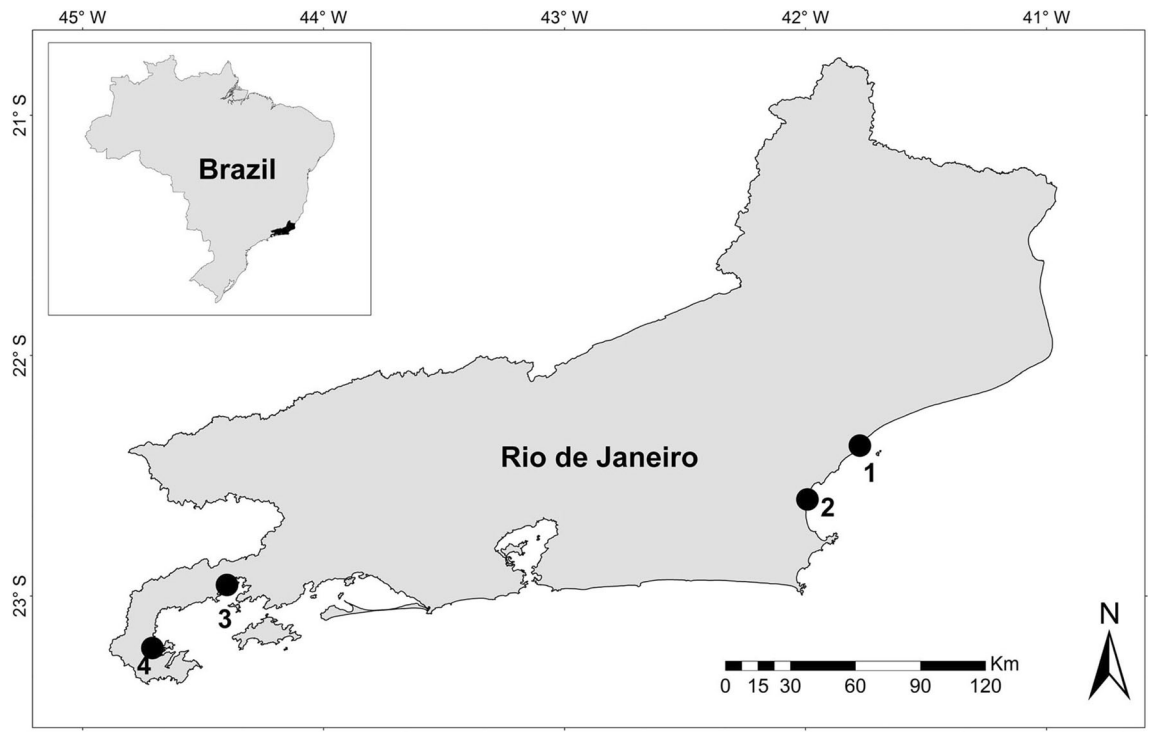

Fig. 1 Map of the sampled estuaries in Rio de Janeiro, Brazil. 1, Macaé river estuary; 2, São João river estuary; 3, Bracuí river estuary; 4, Perequê-Açu river estuary

using Image Pro Plus v. 6.1 (Media Cybernetics, Silver Spring, MD, USA). This study's descriptive terminology follows Huys and Boxshall (1991) and Ferrari and Ivanenko (2008).

Molecular analysis

DNA extraction and amplification

Genomic DNA was extracted from whole specimens, which were washed with TE 1× (10 mM Tris-HCl; 1 mM EDTA; pH 8.0) and placed individually in 1.5-mL microtubes containing 40 μL of cell lysis buffer (10 mM Tris pH 8, 50 mM KCl, 0.5% Tween 20); 20 μg/mL of proteinase K was added to the mixture, following the protocol of Lee and Frost (2002) with some modifications. The material was incubated at 65 °C for 1 h. Then, the samples were heated at 95 °C for 15 min, followed by centrifugation at 13,400 rpm for 10 min. The obtained DNA samples were stored at −20 °C until further analysis. For PCR reactions, 1–2 μL of the extract was used. An ~700-bp fragment of the mtCOI gene was amplified by PCR using the forward and reverse primers L1384 (GGTCATGTAATCAT AAAGATATTG; Machida et al. 2004) and HCO2198 (TAAACTTCAGGGTGACCAAAAAATCA; Folmer et al. 1994), respectively. PCR reactions were performed in a final volume of 25 μL containing 2.5 μL 10× reaction buffer (50 mM KCl, 75 mM Tris-HCl, and 20 mM $(NH_4)_2SO_4$ at pH 9.0), 1.5 mM $MgCl_2$, 0.3 μM of each primer, 0.2 mM dNTPs (dATP, dTTP, dCTP, and dGTP), 0.05 U/μL Taq recombinant DNA polymerase, 10 μg of the template DNA, and sufficient Milli-Q® water (MilliporeSigma, Burlington, MA, USA) to obtain the final volume. Amplification was performed using a Veriti 96-well thermocycler (Applied Biosystems, Foster City, CA, USA) with the following cycling conditions: initial denaturation at 95 °C for 10 min, followed by 40 cycles of denaturation at 95 °C for 30 s, annealing at 42 °C for 30 s, extension at 72 °C for 1 min, and a final extension at 72 °C for 4 min. The PCR products were visualized by electrophoresis on a 1% agarose/TBE (89 mM Tris, 89 mM H_3BO_3, 2 mM EDTA) gel and then prepared for sequencing using a BigDye Terminator v. 3.1 Cycle Sequencing Kit (Applied Biosystems), using the same primers as those used for the PCR amplifications. The sequences were run on an ABI 3500 Genetic Analyzer capillary DNA sequencer (Applied Biosystems).

Sequence editing and analysis

After sequencing, the results were imported to the Sequencing Analysis Software v6.0 (Applied Biosystems), and sequence quality analysis was performed using electropherograms. Consensus sequences of mtCOI were manually edited by comparing the aligned sequences for the forward and reverse strands using Geneious Prime 2019.1 (Biomatters Ltd, Auckland, New Zealand; Larkin et al. 2007). A basic local alignment search tool (BLAST; Altschul et al. 1990) was used with a network service (http://www.ncbi.nlm.nih.gov/) to search for instances of sequence homology in the *GenBank* nucleotide database. Sequences were deposited in *GenBank* with the accession numbers MN444035 and MN444036 (*Paracalanus brasiliensis* sp. nov.) and MN719030 to MN719034 (*Bestiolina brasiliensis* sp. nov.; Table 1).

A 640-bp gene fragment from *Paracalanus brasiliensis* sp. nov. was aligned with the selected sequences used in a previous study of the *Paracalanus parvus* species complex (Cornils and Held 2014; see Supplementary Materials 1 and 2). For *Bestiolina brasiliensis* sp. nov., a 642-bp gene fragment was aligned with all 33 published COI *Bestiolina* sequences (*GenBank*, accessed on June 17, 2019). Alignments and a phylogenetic tree based on maximum likelihood (ML) were built with ClustalW v. 2.0 (Kumar et al. 2016) using MEGA7 (Kumar et al. 2016). In the ML analysis, a general time-reversible (GTR) model was chosen as the nucleotide substitution model (Tavaré 1986) with a proportion of invariable sites, a correction of different site substitution GAMMA rates, and the generation of 1000 bootstrap replicates. Additional *Bestiolina* and *Paracalanus* species sequences present in the NCBI database were incorporated to construct the ML tree (Table 1), and *Acrocalanus gracilis* Giesbrecht, 1888 (JQ911965), and *Acrocalanus longicornis* Giesbrecht, 1888 (JQ911966), were selected to form the outgroups for the *Bestiolina* phylogenetic analysis. Clade support is indicated at the top of the knot of the consensus tree branches. Pairwise genetic distances were also calculated with MEGA7 using the uncorrected p distances for all codon positions.

Results

Systematics

Class Hexanauplia Oakley, Wolfe, Lindgren, & Zaharof, 2013
Subclass Copepoda Milne Edwards, 1840
Order Calanoida G.O. Sars, 1903
Family Paracalanidae Giesbrecht, 1893
Genus *Paracalanus* Boeck, 1865
Paracalanus brasiliensis sp. nov.
Genus *Bestiolina* Andronov, 1991
Bestiolina brasiliensis sp. nov.

Table 1 Information on COI sequences of the *Paracalanus parvus* species group and *Bestiolina* species published in GenBank

Genus	Species	Accession numbers	Location	Remarks
Bestiolina	*Bestiolina similis*	JQ911968	Kaneohe bay, Hawaii	Cornils and Blanco-Bercial (2013)
	Bestiolina similis	KC594120	Kaneohe bay, Hawaii	Jungbluth and Lenz (2013)
	Bestiolina similis	KC594121	Kaneohe bay, Hawaii	Jungbluth and Lenz (2013)
	Bestiolina similis	KC594122	Kaneohe bay, Hawaii	Jungbluth and Lenz (2013)
	Bestiolina similis	KC594123	Kaneohe bay, Hawaii	Jungbluth and Lenz (2013)
	Bestiolina similis	KC594124	Kaneohe bay, Hawaii	Jungbluth and Lenz (2013)
	Bestiolina similis	KC594125	Kaneohe bay, Hawaii	Jungbluth and Lenz (2013)
	Bestiolina similis	KC594126	Kaneohe bay, Hawaii	Jungbluth and Lenz (2013)
	Bestiolina similis	KC594127	Kaneohe bay, Hawaii	Jungbluth and Lenz (2013)
	Bestiolina similis	KC594128	Kaneohe bay, Hawaii	Jungbluth and Lenz (2013)
	Bestiolina similis	KT149367	South West Coast of India	Unpublished
	Bestiolina similis	KT149368	South West Coast of India	Unpublished
	Bestiolina similis	KP068660	South West Coast of India	Unpublished
	Bestiolina similis	AB679172	Palau, Micronesian	Unpublished
	Bestiolina similis	AB679173	Palau, Micronesian	Unpublished
	Bestiolina similis	AB679174	Palau, Micronesian	Unpublished
	Bestiolina similis	AB679175	Palau, Micronesian	Unpublished
	Bestiolina similis	AB679176	Palau, Micronesian	Unpublished
	Bestiolina similis	AB679177	Palau, Micronesian	Unpublished
	Bestiolina similis	AB679178	Palau, Micronesian	Unpublished
	Bestiolina similis	AB679179	Palau, Micronesian	Unpublished
	Bestiolina similis	AB679180	Palau, Micronesian	Unpublished
	Bestiolina similis	AB679181	Palau, Micronesian	Unpublished
	Bestiolina similis	AB679182	Palau, Micronesian	Unpublished
	Bestiolina similis	AB679183	Palau, Micronesian	Unpublished
	Bestiolina similis	AB679184	Palau, Micronesian	Unpublished
	Bestiolina similis	AB679185	Palau, Micronesian	Unpublished
	Bestiolina similis	AB679186	Palau, Micronesian	Unpublished
	Bestiolina similis	AB679187	Palau, Micronesian	Unpublished
	Bestiolina similis	AB679188	Palau, Micronesian	Unpublished
	Bestiolina sp.	KC784343	East China Sea, Changjiang river estuary	Unpublished
	Bestiolina sp.	KC784349	East China Sea, Changjiang river estuary	Unpublished
	Bestiolina sp.	JQ911969	Indonesia, SW Sulawesi	Cornils and Blanco-Bercial (2013)
	Bestiolina brasiliensis sp. nov.	MN719030	Bracuí estuary (1), Rio de Janeiro, Brazil	Developed
	Bestiolina brasiliensis sp. nov.	MN719031	Bracuí estuary (2), Rio de Janeiro, Brazil	Developed
	Bestiolina brasiliensis sp. nov.	MN719032	Macaé estuary, Rio de Janeiro, Brazil	Developed
	Bestiolina brasiliensis sp. nov.	MN719033	Perequê-Açú estuary, Rio de Janeiro, Brazil	Developed
	Bestiolina brasiliensis sp. nov.	MN719034	São João estuary, Rio de Janeiro, Brazil	Developed
Acrocalanus	*Acrocalanus gracilis*	JQ911965	SW Sulawesi, Indonesia	Cornils and Blanco-Bercial (2013)
	Acrocalanus longicornis	JQ911966	Atlantic Ocean, Tropical Eastern Atlantic Ocean	Cornils and Blanco-Bercial (2013)
Paracalanus	*Paracalanus indicus*	KF715899	Indian Ocean, Thailand, Similan Islands	Cornils and Held (2014)
	Paracalanus indicus	KF715902	Coral Sea, Australia	Cornils and Held (2014)
	Paracalanus indicus	KF715903	Coral Sea, Australia	Cornils and Held (2014)
	Paracalanus indicus	KF715904	SW Sulawesi, Indonesia	Cornils and Held (2014)
	Paracalanus indicus	KF715989	Indian Ocean: Scott Reef, Australia	Cornils and Held (2014)

Table 1 (continued)

Genus	Species	Accession numbers	Location	Remarks
	Paracalanus indicus	KC287774	SW Pacific: Australia	Unpublished
	Paracalanus nanus	KF715942	Mediterranean Sea	Cornils and Held (2014)
	Paracalanus nanus	KF715943	Mediterranean Sea	Cornils and Held (2014)
	Paracalanus parvus	KC287798	Akkeshi Bay, Japan	Unpublished
	Paracalanus parvus	KC784345	Changjiang river estuary, China	Unpublished
	Paracalanus parvus	EU599545	Chinese coastal	Unpublished
	Paracalanus parvus	KF715875	North Sea, Helgoland	Cornils and Held (2014)
	Paracalanus parvus	KF715881	Baltic sea, Kattegat, Denmark	Cornils and Held (2014)
	Paracalanus quasimodo	KF715944	Atlantic Ocean: Mauritania	Cornils and Held (2014)
	Paracalanus quasimodo	KF715949	Mediterranean Sea, Algeria	Cornils and Held (2014)
	Paracalanus quasimodo	KF715958	Mediterranean Sea, Algeria	Cornils and Held (2014)
	Paracalanus tropicus	KF715919	Atlantic Ocean, tropical eastern	Cornils and Held (2014)
	Paracalanus tropicus	KF715924	Atlantic Ocean, tropical eastern	Cornils and Held (2014)
	Paracalanus tropicus	KF715931	Atlantic Ocean, tropical eastern	Cornils and Held (2014)
	Paracalanus tropicus	KF715936	Gulf of Aqaba, Red Sea	Cornils and Held (2014)
	Paracalanus tropicus	KF715937	SW Sulawesi, Indonesia	Cornils and Held (2014)
	Paracalanus tropicus	KF715939	Indian Ocean: Red Sea	Cornils and Held (2014)
	Paracalanus sp.	KF715988	Coral Sea: Australia	Cornils and Held (2014)
	Paracalanus sp. B	KF715992	Pacific Ocean: Australia, Melbourne	Cornils and Held (2014)
	Paracalanus sp. B	KF715996	Pacific Ocean: Australia, Melbourne	Cornils and Held (2014)
	Paracalanus sp. C	KF715882	Pacific Ocean: Northeast, Oregon	Cornils and Held (2014)
	Paracalanus sp. C	KF715883	Pacific Ocean: Northeast, Oregon	Cornils and Held (2014)
	Paracalanus sp. C	KF715887	Pacific Ocean: Northeast, Oregon	Cornils and Held (2014)
	Paracalanus sp. D	KF715977	Chile	Cornils and Held (2014)
	Paracalanus sp. D	KF715978	Chile	Cornils and Held (2014)
	Paracalanus sp. D	KF715979	Comau fjord, Chile	Cornils and Held (2014)
	Paracalanus sp. E	KF715983	Atlantic Ocean: Mar del Plata, Argentina	Cornils and Held (2014)
	Paracalanus sp. E	KF715984	Atlantic Ocean: Mar del Plata, Argentina	Cornils and Held (2014)
	Paracalanus sp. E	KF715985	Atlantic Ocean: Mar del Plata, Argentina	Cornils and Held (2014)
	Paracalanus sp. E	KF715986	Atlantic Ocean: Mar del Plata, Argentina	Cornils and Held (2014)
	Paracalanus sp. E	KF715987	Atlantic Ocean: Mar del Plata, Argentina	Cornils and Held (2014)
	Paracalanus sp. F	KF715888	Atlantic Ocean Northwest	Cornils and Held (2014)
	Paracalanus sp. F	KF715889	Atlantic Ocean Northwest: Gulf of Maine	Cornils and Held (2014)
	Paracalanus sp. F	KF715891	Atlantic Ocean Northwest	Cornils and Held (2014)
	Paracalanus sp. F	KF715967	Atlantic Ocean tropical eastern	Cornils and Held (2014)
	Paracalanus sp. F	KF715970	Atlantic Ocean: South Africa	Cornils and Held (2014)
	Paracalanus sp. F	KF715975	New Zealand: Foveaux Strait	Cornils and Held (2014)
	Paracalanus brasiliensis sp. nov.	MN444035	Perequê-Açú estuary, Rio de Janeiro, Brazil	Developed
	Paracalanus brasiliensis sp. nov.	MN444036	Perequê-Açú estuary, Rio de Janeiro, Brazil	Developed

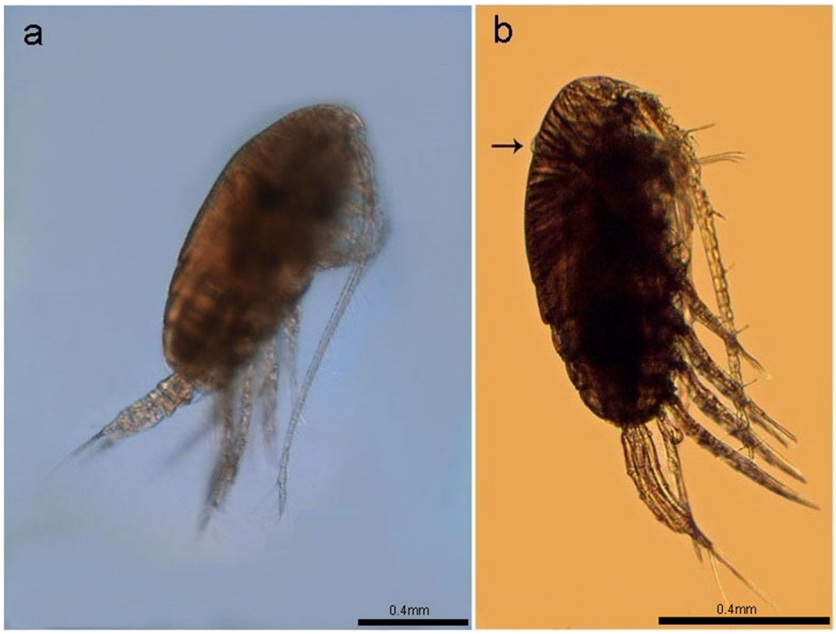

Fig. 2 *Paracalanus brasiliensis* sp. nov. **a** Female, lateral view (holotype MNRJ-028868). Differential interferential phase contrast (DIC) micrographs; **b** male, lateral view showing cephalic hump (allotype MNRJ-028869). Optical microscope photomicrograph

Paracalanus brasiliensis sp. nov.
http://zoobank.org/01D9E68A-00CA-4065-849B-3331F1CD79E0
(Figs. 2, 3, 4, 5, 6, and 7; Table 2)

Material examined (type material) Holotype: MNRJ-028868 adult females were undissected. Total length (TL, measured from the tip of the rostrum to the posterior margin of the caudal rami) 0.58 mm; collected on July 28, 2014, in the Bracuí estuary, Rio de Janeiro, Brazil. Allotype: MNRJ-028869, adult male, undissected. TL 0.67 mm; collected on September 24, 2014, in Bracuí estuary, Rio de Janeiro, Brazil. Paratypes: DZUFRJ Copepoda-39657, three adult females, each dissected and mounted on slides, from the Macaé estuary (August 3, 2013, Rio de Janeiro, Brazil). These specimens were studied using a Stemi SV6 stereomicroscope and an SZX-ILLB2-100 stereomicroscope; DZUFRJ Copepoda-39655, 27 adult female undissected, same locality and date (TL 0.48–0.67 mm, mean 0.57 mm, SD ± 0.06 mm); two females processed for SEM micrographs and 29 adult females undissected (TL 0.48–0.58 mm, mean 0.54 mm, SD ± 0.04 mm), same locality and date of the holotype (C. Dias, F. Vieira-Menezes, and S. Bonecker). DZUFRJ Copepoda-45968, two adult males, each dissected and mounted on slides, at the same locality and date. These specimens were studied using a Stemi SV6 stereomicroscope and an SZX-ILLB2-100 stereomicroscope; DZUFRJ Copepoda-39656, seven adult males were undissected. TL 0.39–0.45 mm, mean 0.41 mm, SD ± 0.02 mm; same locality and date.

Complementary observations DZUFRJ Copepoda-39658, 30 adult females collected in the Perequê-Açú (June 2, 2014, TL 0.48–0.58 mm) and DZUFRJ Copepoda-39659, 30 adult females collected in the São João (July 26, 2014, TL 0.51–0.70 mm) estuaries, Rio de Janeiro, Brazil.

Etymology The specific name refers to Brazil, the country in which this species was collected.

Type locality The Bracuí River Basin is located in the southern region of Rio de Janeiro. The basin has a drainage area of 185 km^2 (COPPETEC 2014). The river runs 24 km to its mouth located in Ilha Grande Bay (Angra dos Reis, Rio de Janeiro; Francisco and Carvalho 2004; Francisco and Oliveira 2009). The estuary is shallow (1–5 m deep) and classified as microtidal (tide range <2 m), with semidiurnal tides that range from 0.5 to 1.0 m during neap and spring tides, respectively (CHM 2016). The climate is classified as tropical super-humid and warm (Silva Soares et al. 2005; Salgado et al. 2007; Cronemberger 2014) because of the Serra do Mar orographic barrier. The mean temperature and annual rainfall are over 18 °C and 2,000 mm, respectively (Silva Soares et al. 2005; Salgado et al. 2007; Cronemberger 2014). The bay's hydrographic region has one of the highest rainfall indices in Rio de Janeiro, with the spatial distribution of its precipitation influenced by the rugged topography present (Farias et al. 2017).

The description was made using the following main differential diagnoses for the *Paracalanus* species: appearance of rostrum, total number of spines present on the dorsal surface of the exopod and endopodite segments 1–3, and the structure of leg 5.

Description of female (based on the holotype and paratypes) Body slender. Prosome and urosome distinctly separated. The

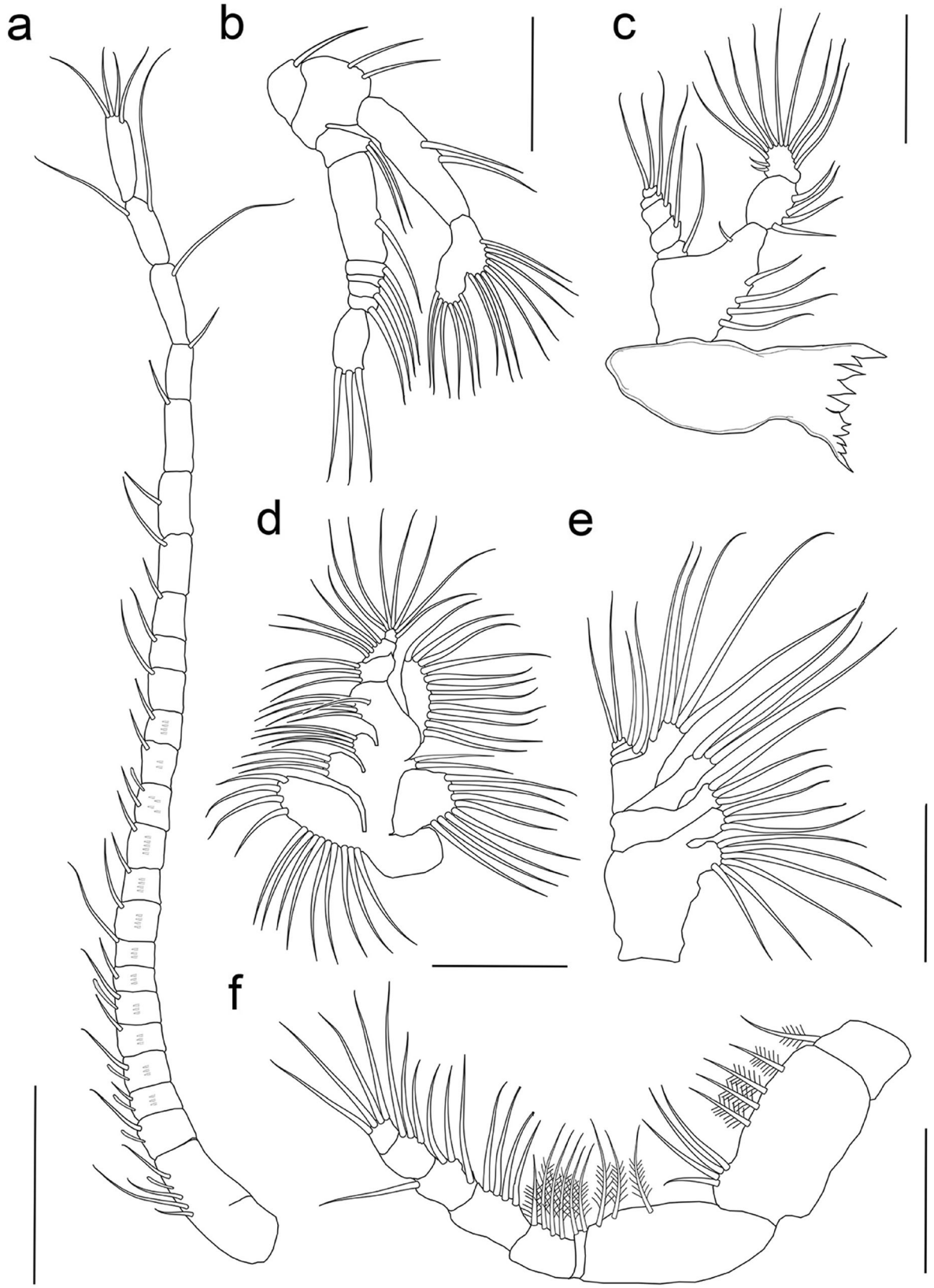

Fig. 3 *Paracalanus brasiliensis* sp. nov. female. **a** Antennule (holotype MNRJ-028868, paratypes DZUFRJ Copepoda-39655 and DZUFRJ Copepoda-39657); **b** antenna (holotype MNRJ-028868, paratypes DZUFRJ Copepoda-39655 and DZUFRJ Copepoda-39657); **c** mandible (paratype DZUFRJ Copepoda-39657); **d** maxillule (paratype DZUFRJ Copepoda-39657); **e** maxilla (paratype DZUFRJ Copepoda-39657); **f** maxilliped (holotype MNRJ-028868, paratypes DZUFRJ Copepoda-39655 and DZUFRJ Copepoda-39657). Scale bars: a = 100 μm, b–f = 50 μm

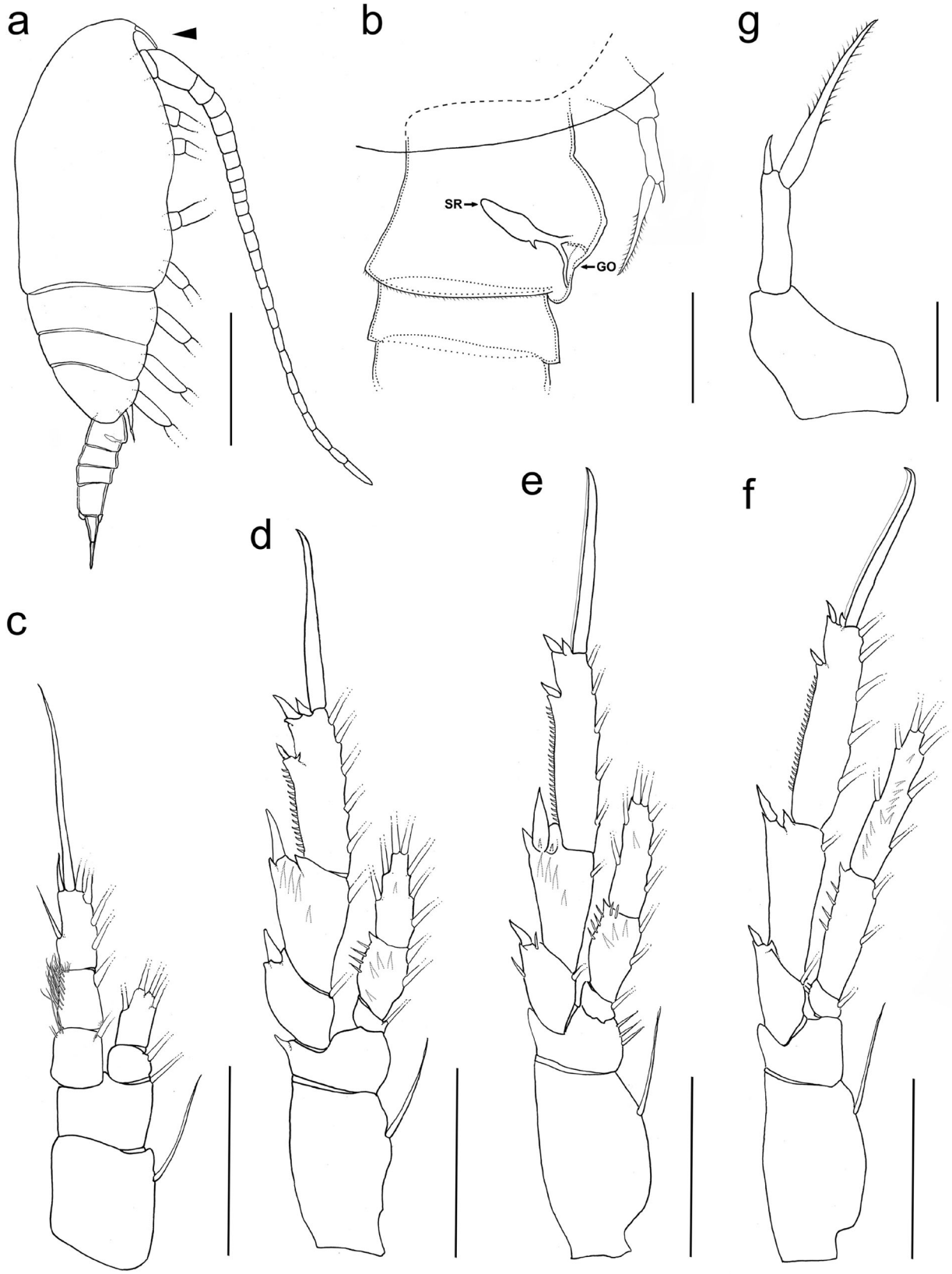

Fig. 4 Schematic drawings of the *Paracalanus brasiliensis* sp. nov. female. **a** Lateral view (holotype MNRJ-028868, paratype DZUFRJ Copepoda-39655), arrow indicating rostrum; **b** genital double somite (holotype MNRJ-028868, paratypes DZUFRJ Copepoda-39655 and DZUFRJ Copepoda-39657), arrow indicating seminal receptacle (SR) and genital operculum (GO); **c** P1; **d** P2; **e** P3; **f** P4; **g** P5 (holotype MNRJ-028868, paratypes DZUFRJ Copepoda-39655 and DZUFRJ Copepoda-39657). Scale bars: a = 170 μm, b = 30 μm, c–f = 65 μm, g = 20 μm

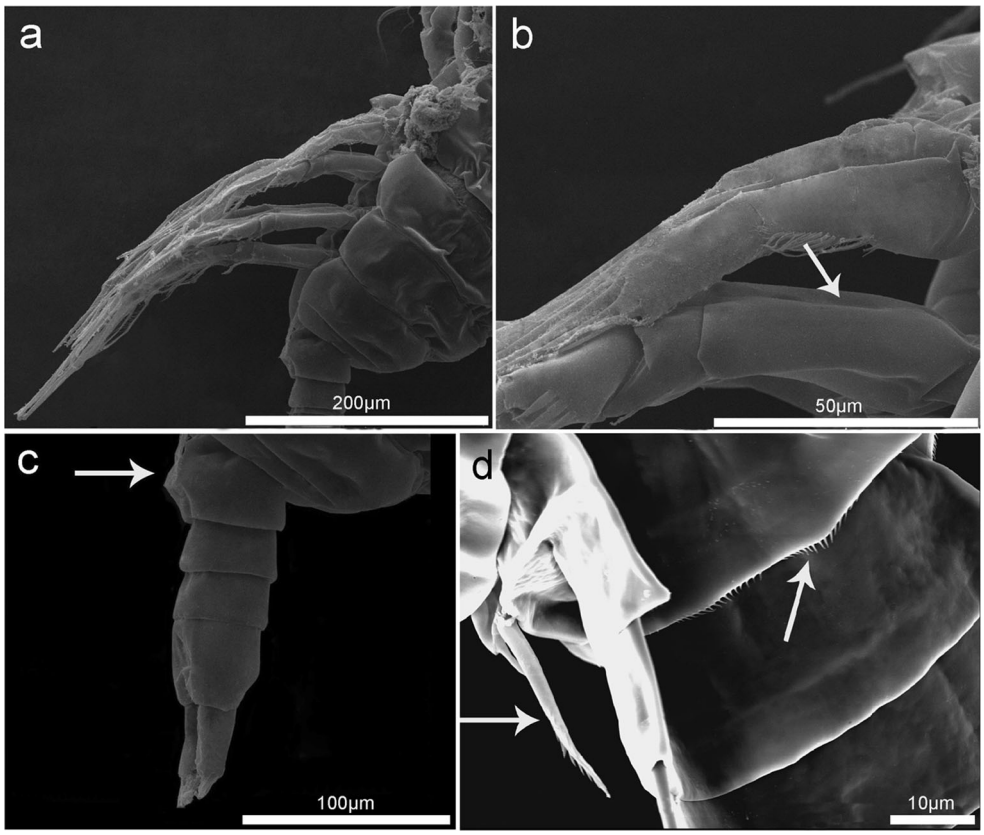

Fig. 5 *Paracalanus brasiliensis* sp. nov. female (paratype DZUFRJ Copepoda-39655). **a** P1 to P4; **b** detail of the P1 and P2 coxopodites without spinules; **c** urosome showing genital double somite, lateral view; **d** P5 from another female. Scanning electron micrograph (SEM)

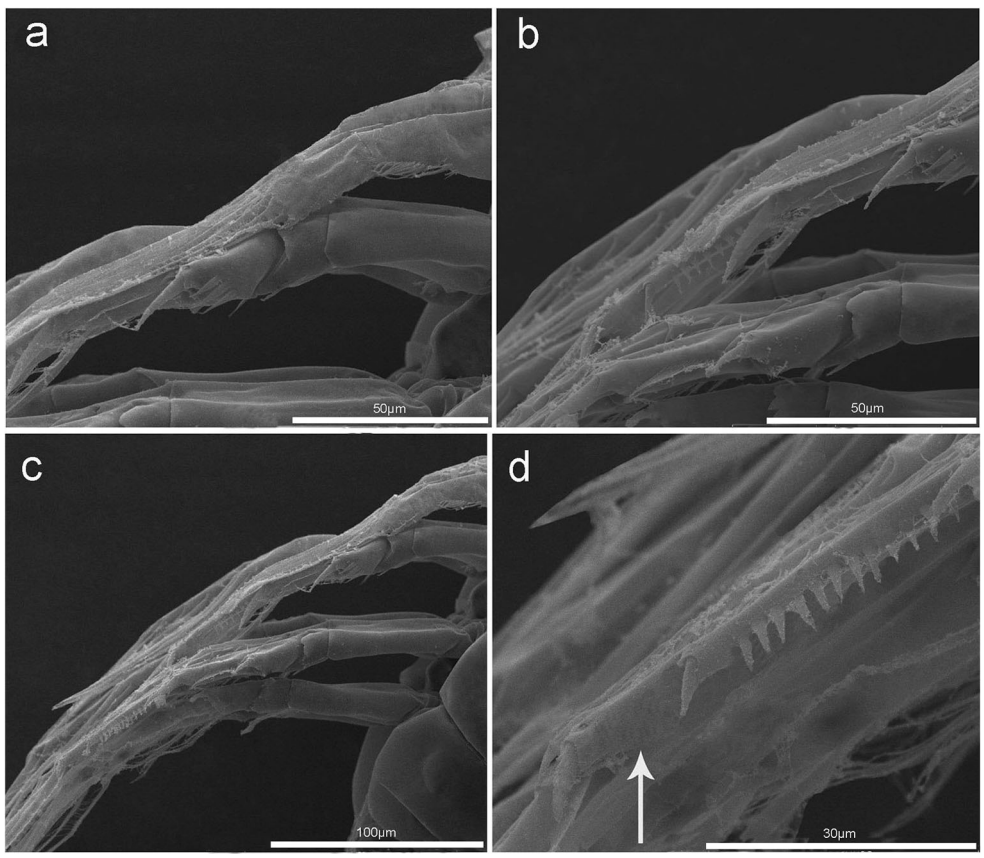

Fig. 6 *Paracalanus brasiliensis* sp. nov. micrographs showing the coxopodite and the distal margin without spinules of the swimming legs of two females (paratype DZUFRJ Copepoda-39655). **a** P1 with minute spinules in segment 2 of the exopodite and **b** P2 showing the external spine and the spinules in segment 1 of the exopodite; **c** P2–4; **d** arrow indicating absence of a spinule row between the two spines on P4. Scanning electron micrograph (SEM)

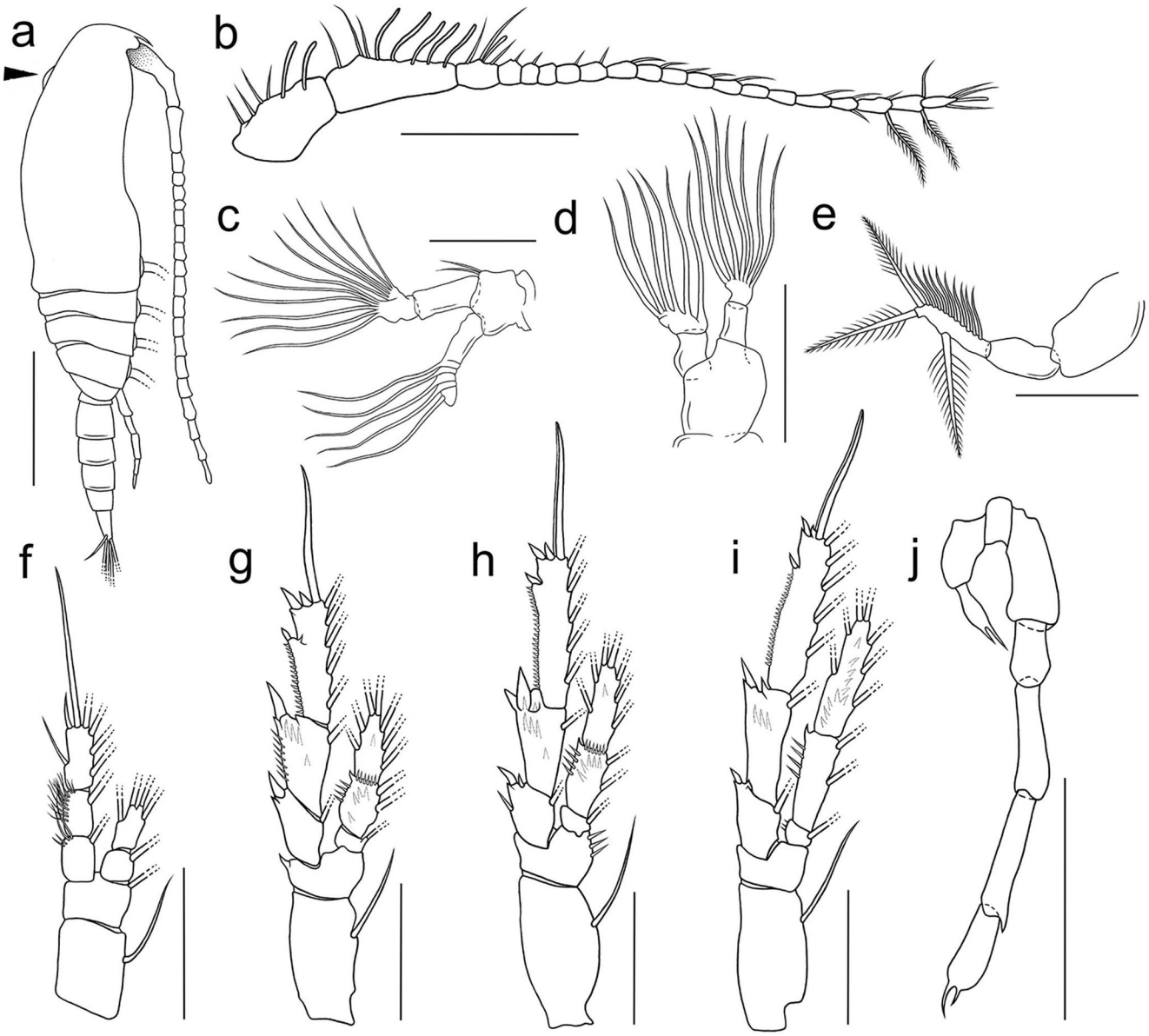

Fig. 7 Schematic drawings of the *Paracalanus brasiliensis* sp. nov. male. **a** Lateral view (allotype MNRJ-028869, paratypes DZUFRJ Copepoda-39656 and DZUFRJ Copepoda-45968), arrow indicating cephalic hump; **b** antennule (allotype MNRJ-028869, paratypes DZUFRJ Copepoda-39656 and DZUFRJ Copepoda-45968); **c** antenna (allotype MNRJ-028869, paratypes DZUFRJ Copepoda-39656 and DZUFRJ Copepoda-45968); **d** mandible (paratype DZUFRJ Copepoda-45968); **e** maxilliped (allotype MNRJ-028869, paratypes DZUFRJ Copepoda-39656 and DZUFRJ Copepoda-45968); **f** P1; **g** P2; **h** P3; **i** P4; **j** P5 (allotype MNRJ-028869, paratypes DZUFRJ Copepoda-39656 and DZUFRJ Copepoda-45968). Scale bars: a = 200 μm, b = 100 μm, c–e = 50 μm, f–i = 65 μm, j = 20 μm

Table 2 Spine and setal formula of legs 1–4 in *Paracalanus brasiliensis* sp. nov.

Leg	Coxa	Basis	Exopodite			Endopodite		
			1	2	3	1	2	3
1	0-1	0-1	0-1	0-1	II,I,4	0-1	1,2,1	-
2	0-1	0-0	I-1	I-1	II,I,5	0-1	0-2	2,2,3
3	0-1	0-0	I-1	I-1	II,I,5	0-1	0-2	2,2,3
4	0-1	0-0	I-1	I-1	II,I,5	0-1	0-2	2,2,3

prosome was three times larger than the urosome. The prosome had the largest amplitude in the middle region (Figs. 2a and 4a). Head fused with the first pedigerous somite; fourth and fifth pedigerous somites separated by indistinct sutures. Antennule shorter than the body, reaching the anterior margin of the caudal rami (Figs. 2a and 4a). Rostrum short, with two thin filaments (Fig. 4a). Urosome 4-segmented (Figs. 4a and 5c). Genital double somite was broader than the length of the urosome (Fig. 5c). Lateral surface without cluster of spinules on either side and with minute denticles on distal margin (Fig. 5d). Seminal receptacles elliptical, with proximal

half narrower than distal half (Fig. 4b), extended dorsally from the genital field. The genital operculum projected ventrally anterior to the seminal receptacles. The anal somite has the same length as the second and third segments (Fig. 4a).

Antennule (Fig. 3a): 25-segmented, extending to the posterior margin of the anal somite. Segments 1 (I) and 2 (II–IV) were partially fused. Segments 3 (V)–24 (XXVI). Apical segment 25 (XXVII–XXVIII) Armature (seta = s) pattern as follows: segments 1 and 2 (I–IV) - 4s + 1 aesthetasc, 3 (V) - 1s + 1 aesthetasc, 4 (VI) - 1s + 1 aesthetasc, 5 (VII) - 1s + 1 aesthetasc, 6 (VIII) - 1s, 7 (XI) - 1s + 1 aesthetasc, 8 (X) - 1s, 9 (XI) - 1s, 10 (XII) - 1s, 11 (XIII) - 1s, 12 (XIV) - 1s, 13 (XV) - 1s + 1 aesthetasc, 14 (XVI) - 1s, 15 (XVII) - 1s, 16 (XVIII) - 1s, 17 (XIX) - 1s, 18 (XX) - 1s, 19 (XXI) - 1s, 20 (XXII) - 1s, 21 (XXIII) - 1s, 22 (XXIV) - 1s, 23 (XXV) - 1s, 24 (XXVI) - 2s, and 25 (XXVII–XXVIII) - 3s + 1 aesthetasc. Segments 4–15 have small spines.

Antenna (Fig. 3b): biramous; coxa and basis clearly separate, bearing 1 and 2 two setae, respectively. Exopodite 7-segmented, slightly longer than endopodite; segment 1 with 2 setae, segments 2–6 with 1 seta each, segment 7 bearing 3 setae apically. Endopodite 2-segmented, first segment with 2 setae, second segment bilobed, with proximal lobe bearing 8 setae of different lengths, and distal lobe bearing 6 setae.

Mandible (Fig. 3c): with cutting edge of gnathobase bearing 9 cuspidate teeth and 1 seta. Palp biramous; basis with 5 setae; exopod 5-segmented, segments 1–4 each with 1 seta, segment 5 bearing 2 apical setae. Endopodite 2-segmented, bearing 4 setae on proximal segment and 11 setae on distal segment.

Maxillule (Fig. 3d): praecoxal arthrite with 13 setae. Coxa with 3 setae on endite; epipodite with 8 setae. Basis with 4 setae on proximal endite and 5 setae on distal endite; basal exite with 2 setae. Exopod bearing 11 lateral setae. Endopodite 3-segmented, first to third segments with 3, 4, and 7 setae, respectively.

Maxilla (Fig. 3e): praecoxa bearing 2 endites; proximal endite with 6 setae, distal with 3 setae; coxa with 2 endites, each armed with 3 setae; basis with a single endite bearing 4 setae and 1 seta laterally. Endopodite 3-segmented with a setal formula of 1, 1, 2.

Maxilliped (Fig. 3f): praecoxa and coxa apparently separate; praecoxa with 1 seta; coxa bearing 1, 3, and 4 setae representing endites, and the setae of the first two endites are spiniforms in the proximal portion; basis bearing 3 spiniform setae in the proximal portion. Endopodite 6-segmented; first to sixth segments bearing 2 spiniform setae in the proximal portion, 4 spiniform setae in the proximal portion, 4, 3+1, 3, and 4 setae, respectively.

Swimming legs 1–4 increase in size posteriorly (Figs. 4c–f and 5a). The spine and setal formula of the swimming legs are shown in Table 2 (Figs. 4c–f and 6a). Coxae not ornamented with spines or spinules (Figs. 4c–f and 5a–b). Legs 1–4 coxae with bristles on the inner border (Fig. 4c–f). Leg 1 basis with a bristle on the inner border (Fig. 4c).

Endopodite 2-segmented in leg 1, 3-segmented in legs 2–4, the posterior margin being ornamented with spines (Fig. 4c–f). The first bristle of the endopodite of legs 2–4 reached the first spine of exopodite segment 3 of the same swimming leg.

Swimming legs 1–4 with 3-segmented exopodites. Last segment of legs 2–4 with rectangular form and spinule row on its margin. This segment has no spinule row in the distal space between the two major spines (Figs. 4c–f and 6b–e).

Leg 5 2-segmented, short, and symmetrical; first segment slightly robust; second segment bearing two thin and unequal terminal spines, the longest one having minute spinules in its distal portion (Figs. 4g and 5d).

Description of male (based on allotype and paratypes) Prosome 5-segmented. Cephalosome bearing a cephalic dorsal hump visible in lateral view. The head completely fused with the first pedigerous somite, and fourth and fifth pedigerous somites were completely separated (Figs. 2b and 7a). Similar to the female, antennule shorter than the body, reaching the distal portion of urosomite 4. Rostrum as in female. Male mouthparts were significantly reduced. Urosome 5-segmented without spinules on the genital somite, anal segment longer than urosomite 4, caudal rami twice as long as wide (Fig. 7a).

Antennule 20-segmented, extending to the distal part of urosomite 4 (Fig. 7b). Ancestral segments (Huys and Boxshall 1991) I–II, III–VI, and VII–VIII fused and protruding. Double apical segment 25 (XXVII–XXVIII). Armature (seta = s) considering ancestral segmentation (in Roman numerals) as follows: segment 1 (I–II) - 4s + 2 aesthetasc, 2 (III–VI) - 3s + 5 aesthetasc, 3 (VII–VIII) - 3s + 1 aesthetasc, 4 (IX–X) - 1s, 5 (XI–XII) - 1s, 6 (XIII) - 0, 7 (XIV) - 1s, 8 (XV) - 1s, 9 (XVI) - 1s, 10 (XVII) - 1s, 11 (XVIII) - 1s, 12 (XIX) - 1s, 13 (XX) - 1s, 14 (XXI) - 0, 15 (XXII) - 0, 16 (XXIII) - 1s, 17 (XXIV) - 2s, 18 (XXV) - 2s, 19 (XXVI) - 2s, 20 (XXVII–XXVIII) - 3s + 1 aesthetasc.

Antenna (Fig. 7c) biramous but atrophied, coxa, and basis completely fused with two setae, proximal segments elongate at the distal segment's expense, exopodite incompletely fused, with 5 setae; the 3 terminal setae present in the female are absent in the male. Endopodite 2-segmented, proximal endopodal segment naked, distal segment with 5 setae about midway of inner margin and with 6 terminal setae.

Mandible (Fig. 7d) coxal gnathobase absent, basis unarmed; exopodite and endopodite 2-segmented, each bearing 6 and 7 setae on the distal segment, respectively.

Maxillule and maxilla vestigial (not drawn). Maxillule significantly reduced, and maxilla presumed to be represented by a knob.

Maxilliped (Fig. 7e) with coxa and basis naked, terminal part not segmented with 3 plumose outer setae and atrophied inner setae.

Swimming legs seta and spine formula and ornamentation generally as in females. Coxae not ornamented with spines or spinules, outer edge of exopod segment 2 of legs

2–4 not serrated (Fig. 7f–i). The swimming legs differ from those of the female in the following aspects: leg 2 exopodite segment 2 with minute spinules along the lateral border; leg 4 exopodite segment 2 with posterior margin ornamented with spines; legs 2–3 endopodite segment 2 with spinules around the distal border, and leg 3 with more spines in the posterior margin than in females. Leg 5 was strongly asymmetrical and uniramous (Fig. 7j). Left P5 5-segmented and extends beyond the distal border of urosome segment 4; basis and exopodite segment 1 unarmed; exopodite segment 4 terminates into the spine. The right leg is 2-segmented and extends beyond the medium portion of the left leg segment 2. Both legs had two thin and unequal terminal spines in the distal segment.

Sequence analysis and phylogenetic inference

Fifty females were identified as *Paracalanus brasiliensis* sp. nov. for molecular analysis (17 from the Bracuí estuary, 13 from the Macaé estuary, 2 from the Perequê-Açu estuary, and 18 from the São João estuary). Only two extractions (from the Perequê-Açu and São João estuaries) were sequenced.

Sequences from *Paracalanus brasiliensis* sp. nov. (*GenBank* Accession numbers: MN444035 and MN444036) aligned with the lineage "*Paracalanus* sp. E" (*GenBank* Accession numbers KF715983–KF715987; Cornils and Held 2014), which included specimens from the Southwest Atlantic (Supplementary Materials 1 and 2).

Intraspecific p distances within the lineage "*Paracalanus* sp. E" and *Paracalanus brasiliensis* sp. nov. ranged between 0 and 0.009 and were therefore well below the assumed genetic divergence threshold in COI for distinct copepod species (Bucklin et al. 1999). For all other sequences of the *P. parvus* species complex, the uncorrected p distances varied between 0.134 and 0.178 (alignment provided as Supplementary Material 1). Thus, we conclude that the sequences from lineage "*Paracalanus* sp. E" from Cornils and Held (2014) also belongs to the newly described species *Paracalanus brasiliensis* sp. nov.

***Bestiolina brasiliensis* sp. nov.**

http://zoobank.org/C4010E14-F38F-4711-AB66-DD4D2F595113

(Figs. 8, 9, 10, 11, 12, 13, 14, 15, 16, and 17; Table 3)

Material examined (type material) Holotype: MNRJ-028870, adult females were undissected. TL 0.52 mm; collected on July 28, 2014, in the Bracuí estuary (22° 57′ 12″ S, 44° 24′ 05″ W), Rio de Janeiro, Brazil. Allotype: MNRJ-028871, adult male, undissected. TL 0.40 mm; collected on February 9, 2015, in the Bracuí estuary, Rio de Janeiro, Brazil. Paratypes: DZUFRJ Copepoda-45969, three adult females, each dissected and mounted on slides, at the same locality and date. These specimens were studied using a Stemi SV6 stereomicroscope and an SZX-ILLB2-100 stereomicroscope; DZUFRJ Copepoda-39660, two adult females were processed for SEM micrographs, and 26 adult females were left undissected. TL 0.44–0.53 mm, mean 0.48 mm, SD ± 0.02 mm, same locality and date (C. Dias and F. Vieira-Menezes); DZUFRJ Copepoda-45970, two adult males, each one dissected and mounted on slides. Organisms were studied using a Stemi SV6 stereomicroscope and an SZX-ILLB2-100 stereomicroscope; DZUFRJ Copepoda-29095, two males

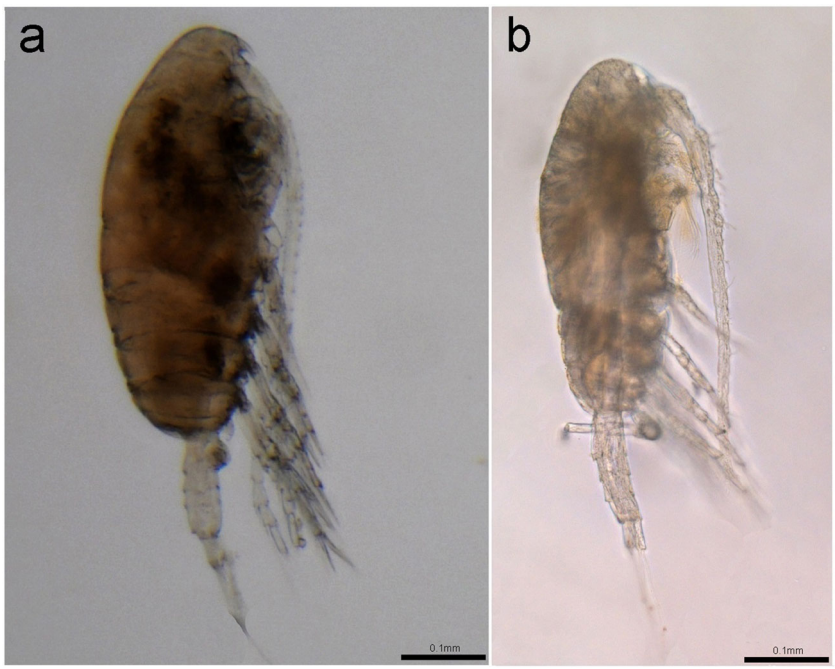

Fig. 8 *Bestiolina brasiliensis* sp. nov. **a** Female, lateral view (holotype MNRJ-028870). Photograph taken on Nikon SMZ25 stereomicroscope; **b** male, lateral view (allotype MNRJ-028871). Differential interferential phase contrast (DIC) micrographs

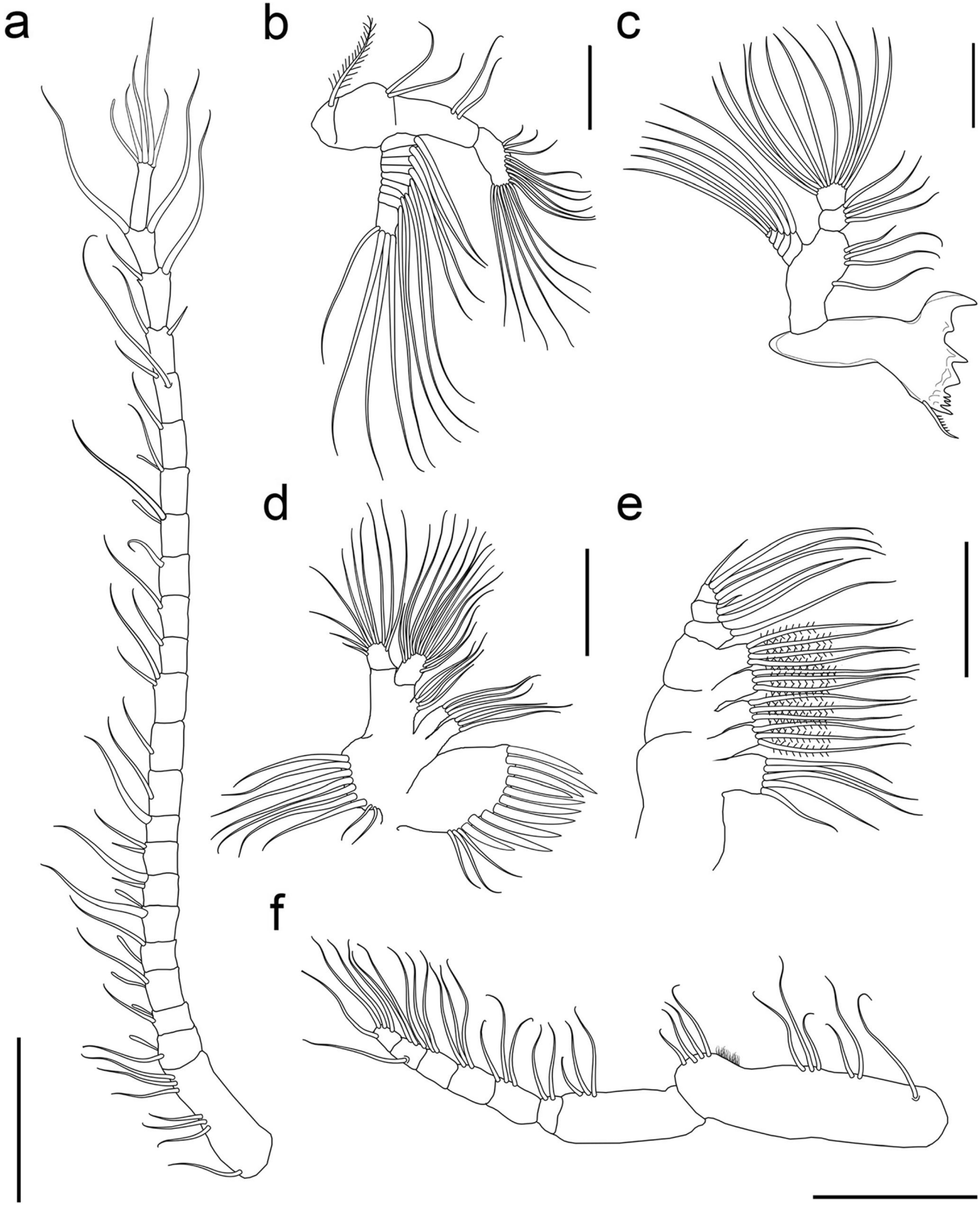

Fig. 9 *Bestiolina brasiliensis* sp. nov. female. **a** Antennule (holotype MNRJ-028870, paratypes DZUFRJ Copepoda-39660 and DZUFRJ Copepoda-45969); **b** antenna (holotype MNRJ-028870, paratypes DZUFRJ Copepoda-39660 and DZUFRJ Copepoda-45969); **c** mandible (paratype DZUFRJ Copepoda-45969); **d** maxillule (paratype DZUFRJ Copepoda-45969); **e** maxilla (paratype DZUFRJ Copepoda-45969); **f** maxilliped (holotype MNRJ-028870, paratypes DZUFRJ Copepoda-39660 and DZUFRJ Copepoda-45969). Scale bars: a = 100 μm, b–f = 50 μm

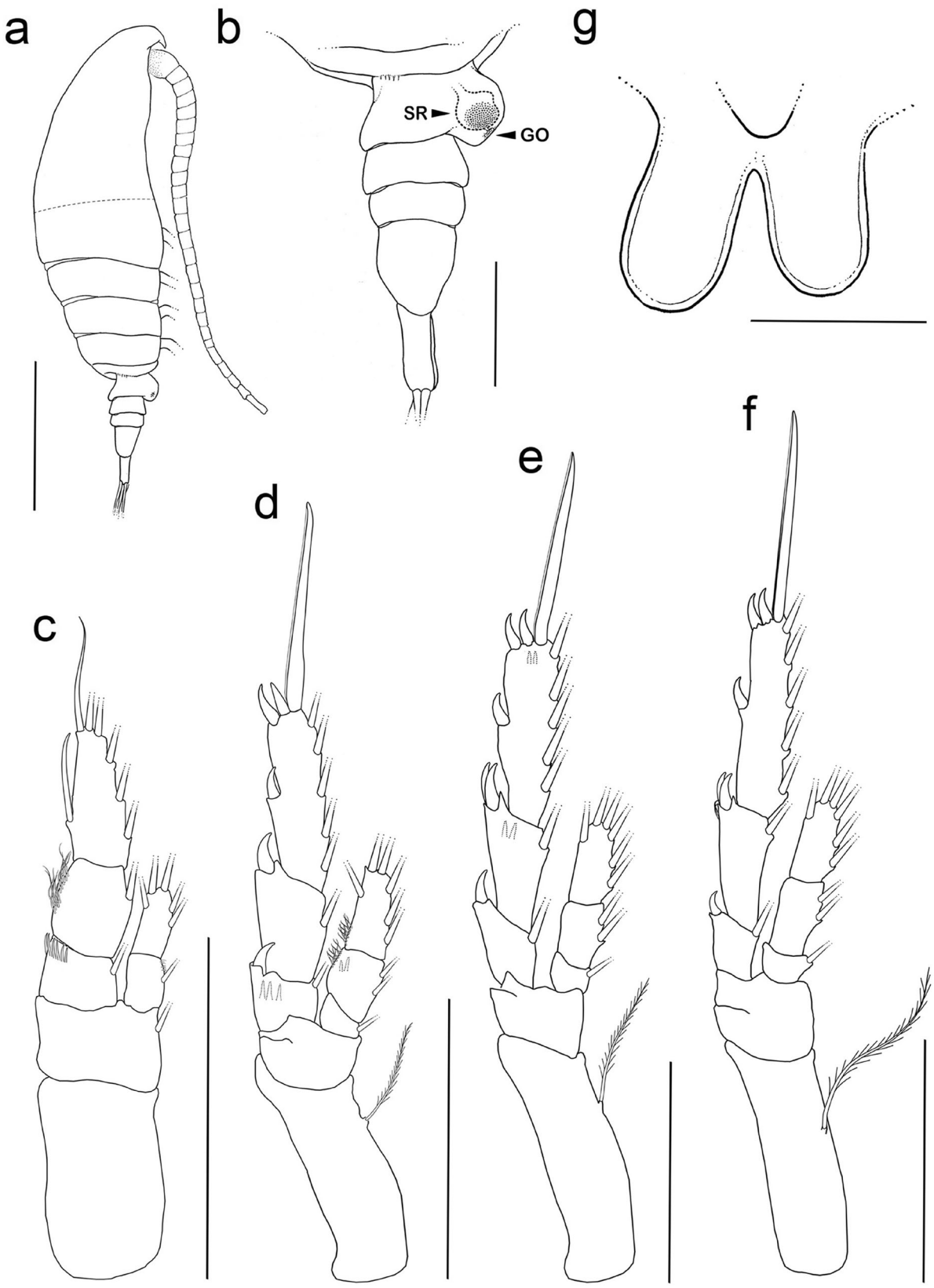

Fig. 10 Schematic drawings of *Bestiolina brasiliensis* sp. nov. female. **a** Lateral view (holotype MNRJ-028870, paratypes DZUFRJ Copepoda-39660 and DZUFRJ Copepoda-45969); **b** urosome (holotype MNRJ-028870, paratypes DZUFRJ Copepoda-39660 and DZUFRJ Copepoda-45969), arrow indicating seminal receptacle (SR) and genital operculum (GO); **c** P1; **d** P2; **e** P3; **f** P4; **g** P5 (holotype MNRJ-028870, paratypes DZUFRJ Copepoda-39660 and DZUFRJ Copepoda-45969). Scale bars: a = 200 μm, b = 50 μm, c–f = 65 μm, g = 20 μm

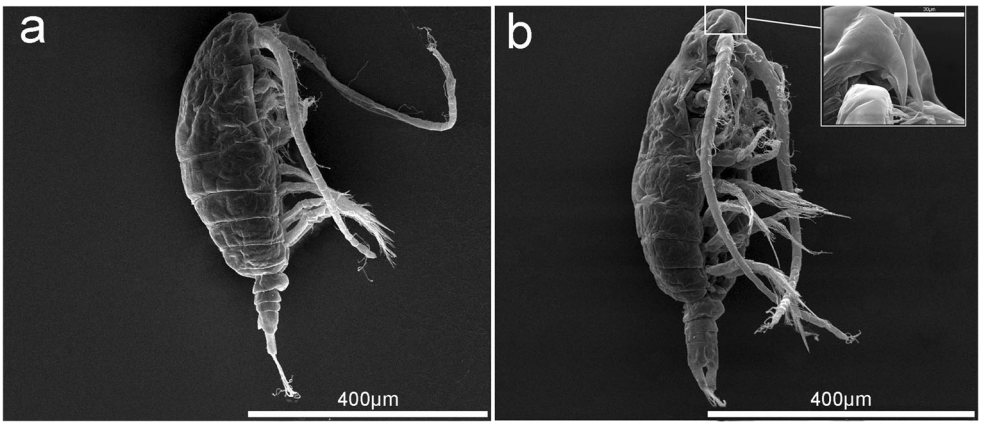

Fig. 11 *Bestiolina brasiliensis* sp. nov. females (paratype DZUFRJ Copepoda-39660). **a** Lateral view; **b** detail of the anterior extremity showing the very robust rostrum. Scanning Electron Micrograph (SEM)

processed for SEM micrographs, and four adult males undissected. TL 0.39–0.45 mm, mean 0.41 mm, SD ± 0.02 mm; same locality and date (C. Dias and F. Vieira-Menezes).

Complementary observations DZUFRJ Copepoda-39662, 34 adult females, collected from the Perequê-Açú estuary (June 2, 2014, TL 0.45–0.57 mm); DZUFRJ Copepoda-39663, 30 adult females from the São João estuary (July 26, 2014, TL 0.43–0.60 mm); and DZUFRJ Copepoda-39664, 30 adult females from the Macaé estuary (March 29, 2014, TL 0.54–0.60 mm), Rio de Janeiro, Brazil.

Etymology The species name refers to Brazil, the country in which the genus was first reported.

Type locality The same as that of *Paracalanus brasiliensis* sp. nov.

The description was made using the following main differential diagnoses for the *Bestiolina* species: rostral projections, presence or absence of spinule rows on the margin of the fifth pedigerous somite, swimming-leg ornamentation, and caudal setae.

Description of female (based on the holotype and paratypes) Body robust, widest at pedigerous somite 1; anterior end of cephalosome rounded, tapering distally (Figs. 8a and 11a–b). Well-developed rostral projections (Fig. 11b). Cephalosome and pedigerous somite 1 were separated by complete sutures (Figs. 10a and 11a). The fourth and fifth pedigerous somites completely separated (Fig. 10a); distal margin of the fifth pedigerous somite rounded with a row of minute spinules (Figs. 10b and 12a–b) in lateral view; exhibits minute spinules in ventral view (Fig. 12a) and minute spinules in the urosome in side view (Fig. 12b). Urosomes with four free somites. The first and second urosomites fused, forming the genital double somite symmetrical in dorsal view, protruding ventrally in lateral view (Figs. 10b and 15a). The genital double somite typically has paired genital apertures, genital operculum, and a pair of rounded colored seminal receptacles appearing in both lateral and ventral views. The genital operculum is located in the ventral-posterior region, anterior to the seminal receptacles (Fig. 15b). In the lateral view, minute spinules on the superior part of the genital double somite. Anal somite slightly longer than the preceding two urosomites combined. Symmetrical caudal rami, almost as long as the anal somite (Figs. 10b and 15a), each ramus contained five caudal setae, one of which was reduced distally at the medial margin.

Antennule (Fig. 9a): 23-segmented, extending to the caudal rami (Fig. 10a). Ancestral segments (Huys and Boxshall 1991) I–IV and XXVII–XXVIII fused. Armature (seta = s, spine = sp) considering ancestral segmentation (in Roman numerals) as follows: I–IV - 7s, V-1s + 1 aesthetasc, VI - 1s + 1 aesthetasc, VII - 1s + 1 aesthetasc, VIII - 1s + 1 aesthetasc, IX - 1s + 1 aesthetasc, X–XI - 1s + sp, XII - 1s + 1 sp, XIII - 1s, XIV - 1s, XV - 1s, XVI-2s, XVII - 1s, XVIII - 1s, XIX - 1s, XX - 1s + 1 aesthetasc, XXI - 1s + 1 aesthetasc, XXII - 1s, XXIII - 2s, XXIV - 1s + 1 sp, XXV - 2s, XXVI - 2s, and XXVII–XXVIII - 4s + 1 aesthetasc.

Antenna (Fig. 9b) is biramous. Coxa with 1 spiniform setae basis with 2 long distal setae Endopod 2-segmented; first segment with 2 unequal setae; second segment bilobate; subterminal lobe with 9 setae; terminal lobe with 6 setae. Exopod 7-segmented, with a setal formula of 1, 3, 1, 1, 1, 1, 4.

Mandible (Fig. 9c): Gnathobase well-developed, cutting edge with short teeth and dorsal seta; basis of palp with 4 subequal setae; endopod 2-segmented, proximal and distal segments with 4 and 11 setae, respectively; exopod 5-segmented, with a setal formula of 1, 1, 1, 1, 2.

Maxillule (Fig. 9d) with praecoxal arthrite carrying 13 setal elements on and around the distal margin. Coxa with 2 endites, each endite with 3 setae; coxal epipodite with 9 setae, 7 setiform, and 2 spiniform. Basis with 4 setae on endite; endopod and exopod with 14 and 11 setae, respectively.

Maxilla (Fig. 9e): praecoxa and coxa incompletely fused, proximal praecoxal endite with 5 setae, distal and coxal endites with 3 spiniform setae in the proximal portion each; basal endite with 4 spiniform setae in the proximal portion.

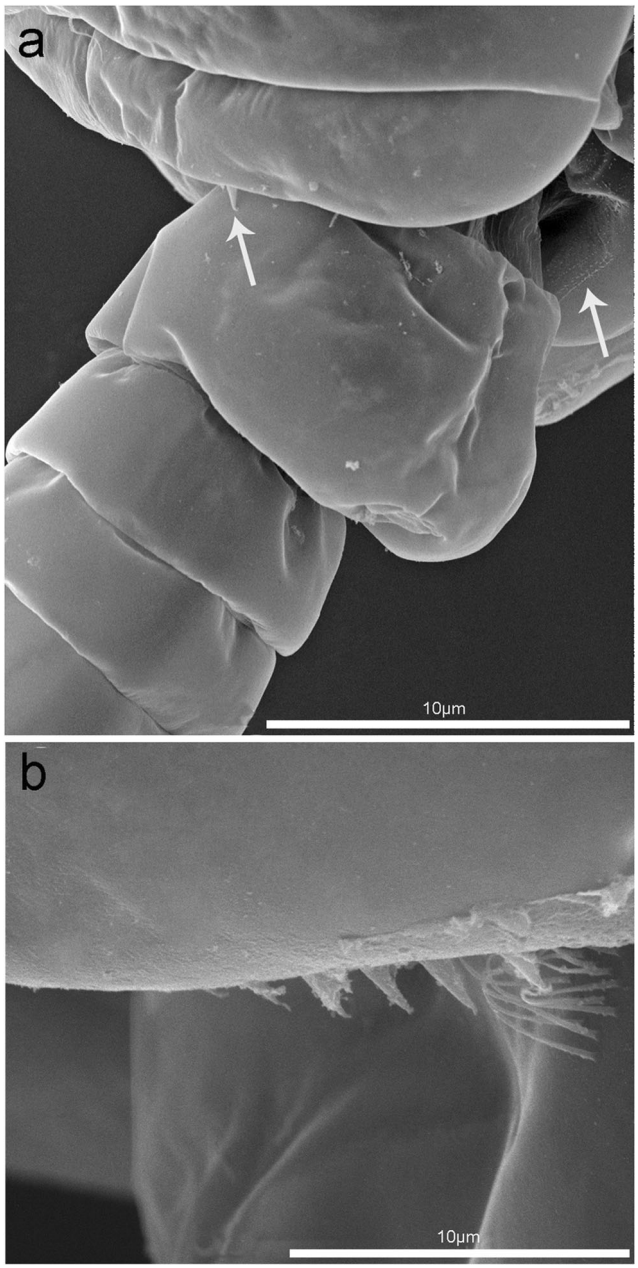

Fig. 12 *Bestiolina brasiliensis* sp. nov. female (paratype DZUFRJ Copepoda-39660). **a** Arrows indicate spinules on the last pedigree somite and the minute spinules in ventral view; **b** detail of the spinules at the distal margin of the prosome. Scanning electron micrograph (SEM)

Endopod 3-segmented; first segment with endite bearing 1 seta; second segment with 3 setae; third segment with 4 setae.

Maxilliped (Fig. 9f): slender, with elongate syncoxa, armed with 4 groups of setal elements, proximally with 1, second with 2, third with 3, and distalmost group with 4 subequal setae; rows of tiny spinules at insertion of third and fourth setal groups. Basis with 3 spiniform setae in the proximal portion Endopod 6-segmented, setal formula of 2, 3, 3, 2, 4, 4. The setae of the endopod 1-segment were spiniform in the proximal portion.

Swimming legs 1–4 increase in size posteriorly, each comprising coxa, basis, and 3-segmented exopodites (Figs. 10c–f and 13a). The spine and setal formulas of the swimming legs are shown in Table 3 (Fig. 10c–f). Leg 1 with 2-segmented endopodite, and legs 2–4 with 3-segmented endopodites. Legs 2–4 coxae with a robust plumose internal bristle (Fig. 10c–f).

Swimming leg 1 with a robust bristle on the basis, reaching the end of the second endopodite segment (Fig. 13c). Exopodite 3-segmented, with the end of the first segment presenting 12 spinules in the outer margin (Fig. 13d). Part of the anterior surface of the base and segments 1, 2, and 3 of the exopodite with tiny and robust spinules (Fig. 13b–c). The second segment ornamented, with a row of long spinules on the outer margin that reaches the last segment (Fig. 13c). The third segment with two slender external spines (Fig. 10c). Endopodite 2-segmented, the first one ornamented with bristles (Figs. 10c and 13b).

Leg 2 with the first exopodite segment ornamented with a row of 3–4 spines (variation between the analyzed specimens) on its posterior face (Fig. 13e–f). Two spinules in the second segment of the exopodite (not shown) and endopodite in the anterior and posterior faces, respectively. Endopodites 2 and 3 with minute spinules (Figs. 10d and 13b).

Leg 3 with the second and third exopodite segments ornamented with two spinules on the anterior and posterior faces, respectively (Figs. 10e and 14a). The third segment's spinules were less conspicuous than those in the second segment (Fig. 14b).

Leg 4 (Fig. 10f) with the second segment of exopodite ornate with two very sharp spinules on its anterior portion (Figs. 10f and 14c).

Leg 5 was reduced, represented by a pair of rounded lobes with slight asymmetry (Figs. 10g and 14d).

Description of male (based on allotype and paratypes) Body slenderer compared with females. Cephalosomes with dorsal humps visible in lateral view (Figs. 16a and 17a, b) and fused with first pedigerous somite as in females (Figs. 8b; 16a; 17a). Fourth and fifth pedigerous somites completely separated, posterolateral margins of fifth pedigerous somite rounded and symmetrical, with a row of minute spinules (Fig. 16a). Rostral projections were thicker but slenderer than in females (Fig. 16a). Urosome 5-segmented, the second longer than the others. Symmetrical caudal branch, approximately 2 times longer than wide; armed with 5 caudal setae, with four distal setae and one distally reduced in the medial border (Figs. 16a and 17d).

Antennule non-geniculate; long and symmetrical, extending about as far as mid-urosome (Fig. 16b); 20-segmented, segment 1 (ancestral segments I–IV), 2 (ancestral segments V–VIII); IX–X and XXVII–XXVIII fused. Segmentation and setation pattern (seta = s) as follows: I–IV–4s, V–VIII–7s, IX–X–2s, XI–

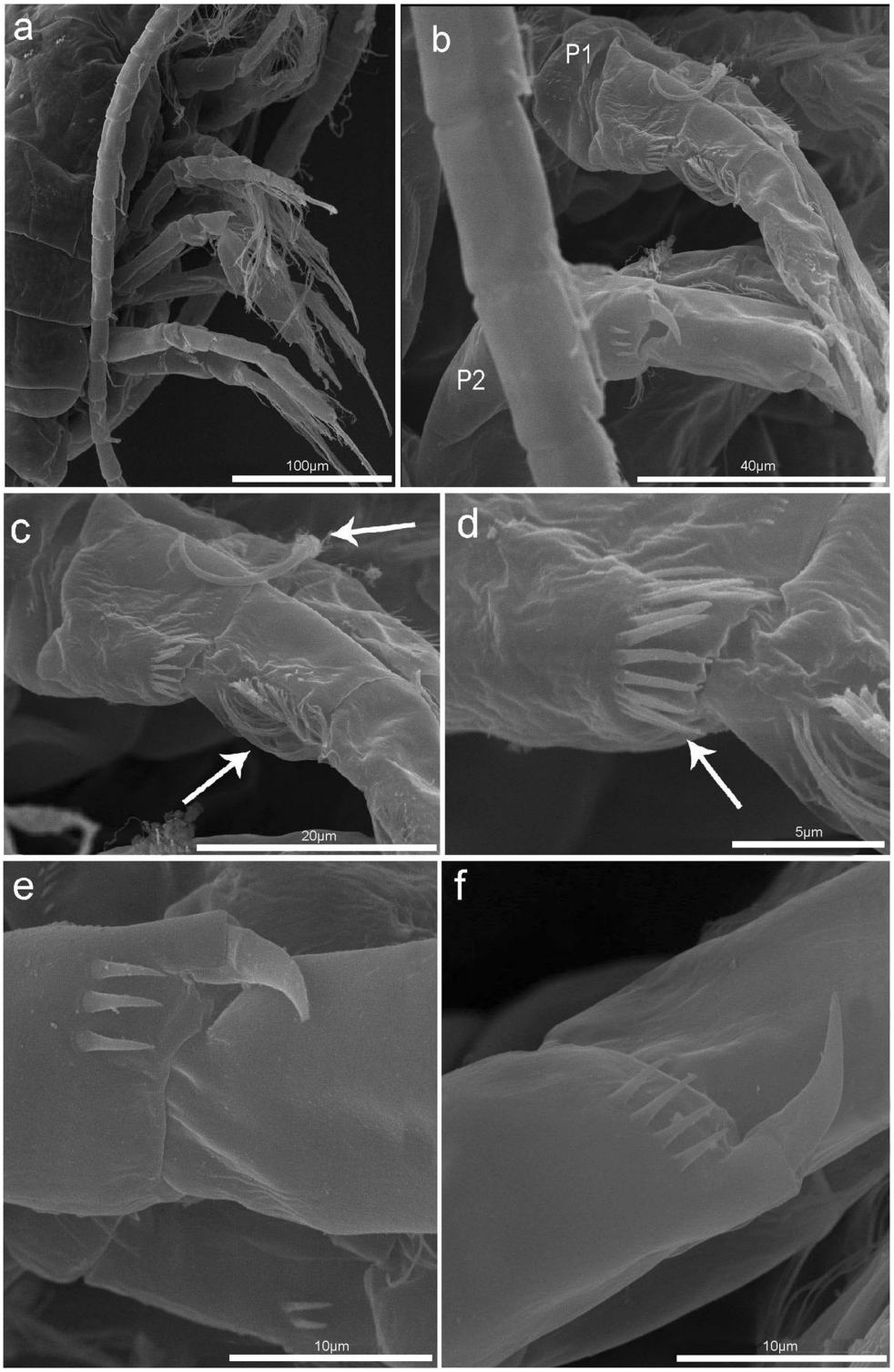

Fig. 13 *Bestiolina brasiliensis* sp. nov. female (paratype DZUFRJ Copepoda-39660). Electron micrographs showing the swimming legs. **a** Increasing size of swimming legs toward P4; **b** ornamentation with P1 and P2 minute spinules, spinules, and spines; **c** detail of basipodite bristle and P1 minute spinules; **d** detail of the spinules in P1; **e**, **f** variation in the number of spinules in the first segment of the P2 exopodite

1s, XII–0, XIII–1s, XIV–1s, XV–0, XVI–0, XVII–0, XVIII–0, XIX–1s, XX–1s, XXI–2s, XXII–0, XXIII–0, XXIV–1s, XXV–2s, XXVI–2s, XXVII–XXVIII–4s + 1 aesthetasc.

Antenna (Fig. 16c) biramous, but atrophied; coxa and basis completely fused, with single seta; endopod 2-segmented, first segment unarmed, second segment bilobed, subterminally with 4 setae and terminally 5 setae; exopod incompletely fused, armed with 5 setae, distal segment small, knob-like, unarmed.

Mandible (Fig. 16d) coxal gnathobase absent, basis unarmed; exopod 2-segmented, with partial suture, armed with 6 setae; endopod 2-segmented, first segment unarmed, second endopodal segment with 8 setae.

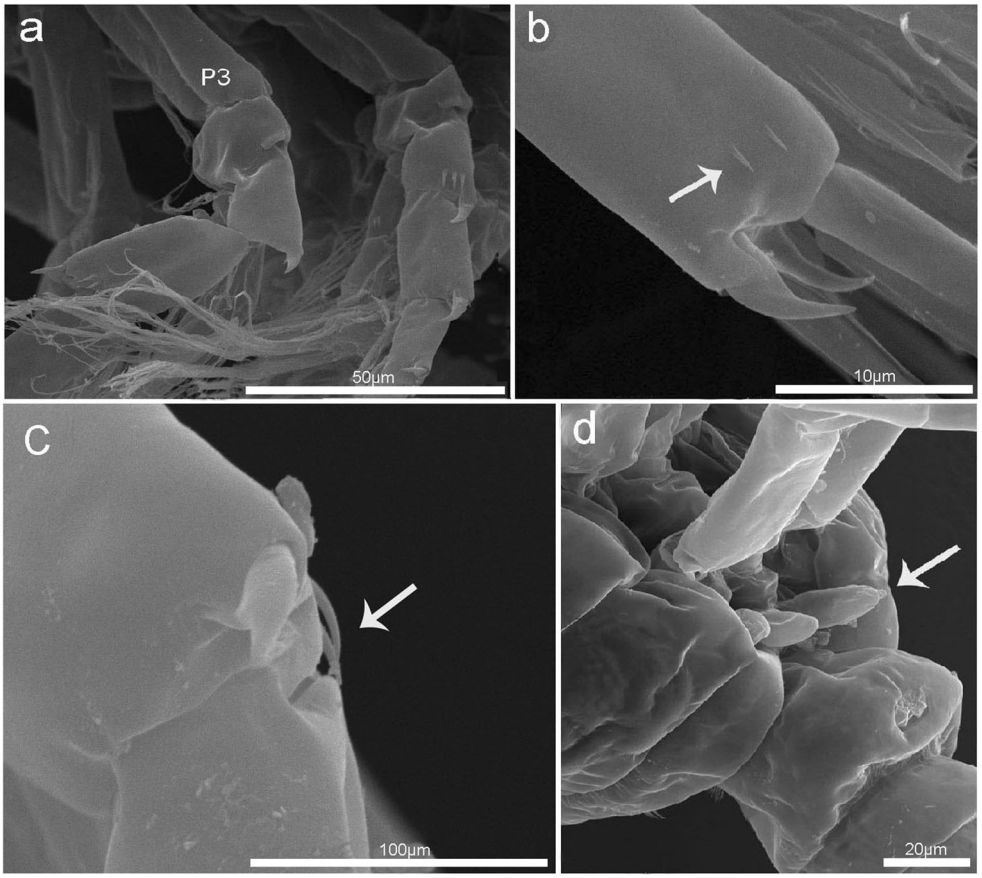

Fig. 14 *Bestiolina brasiliensis* sp. nov. female (paratype DZUFRJ Copepoda-39660). **a** Ornamentation with spines on the second segment of P3 exopodite; **b** spinules on the third segment of the P3 exopodite; **c** spinules on the second segment of P4 exopodite; **d** P5. Scanning electron micrograph (SEM)

Maxillule and maxilla rudimentary (not drawn).

Maxilliped (Fig. 16e) reduced, with 4 segments including long and robust syncoxa without seta, shorter subrectangular basis with single seta, and 2-segmented endopod. First endopodal segment with 3 setae, outermost thick, bipinnate; distal segment with 4 setae, 2 of them thick, bipinnate.

Swimming-leg seta and spine formula and ornamentation generally as in females. Swimming legs differ from those of the female in the following aspects: exopodite terminal seta of legs 1–4 narrower and exopodite outer spines with less curvature than female legs (Fig. 16f–i). Legs 2–3 with exopodite with six spinules on the anterior surface of segment 3, close to the first outer spines (Fig. 16g–h). Swimming leg 5 strongly asymmetrical, right leg rudimentary represented by a rounded lobe as in female (Figs. 16j and 17c–d); left leg 5-segmented, uniramous, as long as urosome (Figs. 16a and 17a). Coxa dilated, basis and first exopodite segment unarmed, exopodite segment 4 with an external latero-distal spine, and distal segment with two unequal spines, one external and exceedingly small, and the other internal, long, and slender (Figs. 16j and 17c).

Sequence analysis and phylogenetic inference

A total of 49 females were used for molecular analysis (four from the Bracuí estuary, four from the Macaé estuary, two from the Perequê-Açu estuary, and 39 from the São João estuary). Five sequences were obtained for the four estuaries (two sequences from Bracuí and one sequence from Macaé, Perequê-Açu, and São João).

The reconstructed ML tree of the *Bestiolina* COI sequences revealed that the sequences of *Bestiolina brasiliensis* sp. nov. (GenBank accession numbers MN719030-MN719034) were different from all other published COI sequences (Supplementary Materials 3 and 4). Uncorrected p distances within *Bestiolina* sp. nov. varied between 0 and 0.006 (alignment in Supplementary Material 3). For all other published *Bestiolina* sequences, the uncorrected p distance ranged from 0.083 to 0.157, which was in the range of the divergence COI threshold for distinct species (Bucklin et al. 1999). However, the maximum likelihood tree of *Bestiolina* spp. yielded several lineages of *Bestiolina similis*, which might be an indication of cryptic speciation within *B. similis* or

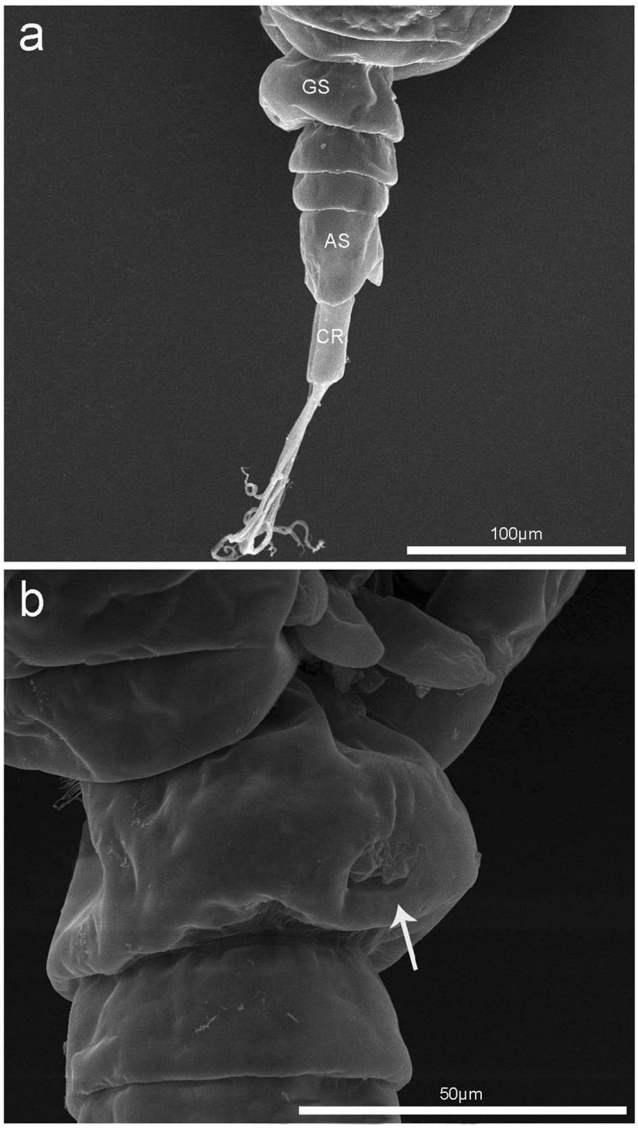

Fig. 15 *Bestiolina brasiliensis* sp. nov. female (paratype DZUFRJ Copepoda-39660). **a** Urosome showing genital double somite (GS), anal somite (AS), and caudal rami (CR), lateral view; **b** seminal receptacles, ventral view. Scanning electron micrograph (SEM)

misidentification. A more comprehensive study of *Bestiolina* species delimitation is needed to resolve these uncertainties.

Discussion

Specimens identified as *Paracalanus* spp. or *Bestiolina similis* collected from estuaries of the central Brazilian coast were reviewed, and unidentified *Paracalanus* spp. adults (females and males) were separated and morphologically analyzed in greater detail. Some morphological differences were found between the specimens classified as either *Paracalanus brasiliensis* sp. nov. or *Bestiolina brasiliensis* sp. nov. and those from the literature of these genera. Taxonomic and genetic analyses of *Paracalanus brasiliensis* sp. nov. and *Bestiolina brasiliensis* sp. nov. specimens suggest that the individuals collected from the four estuaries sampled in this study belong to a new species.

Paracalanus brasiliensis sp. nov

The morphological identification of the *Paracalanus* specimens was based on taxonomic criteria, such as the absence or presence of serration on the outer distal edge of exopodite 3 of swimming legs P2–4 in females. This was the main criterion used to distinguish between *P. parvus*, *P. indicus*, and *P. quasimodo*. The presence or absence of ornamentation on the first basipodite of the swimming legs, as well as the presence or absence of a prominent cephalic dorsal hump on the prosome in males, is also cited as a diagnostic feature (Kasapidis et al. 2018).

Paracalanus brasiliensis sp. nov. has morphological characteristics that differentiate it from the Paracalanidae species belonging to the *P. parvus* species complex found along the Brazilian coast and other parts of the world. These characteristics include the species' swimming legs, the seminal receptacle shape, and total length.

Regarding the structures present in P2–4, females and males of *P. brasiliensis* resemble *P. parvus*, *P. nanus*, *P. intermedius*, and *P. serrulus* in the absence of many posterior surface spinules in the coxopodite, *P. parvus*, *P. intermedius*, and *P. serrulus* in the absence of posterior surface spinules on the basipodite, and *P. parvus* in the absence of serration between the spines of the 3rd articulated exopodite (Table 4; Bradford 1978). According to Bradford (1978), the relationships of both sexes of *P. intermedius* and *P. serrulus* with other members of the *P. parvus* group are difficult to determine because these species have not yet been fully described. Moreover, in a study on the *P. parvus* species complex from the Mediterranean and Black Seas, Kasapidis et al. (2018) demonstrated the difficulty of using routine morphological characters in the discrimination of *Paracalanus* species (*P. parvus*, *P. indicus*, and *P. quasimodo*), especially because of the great variability in the morphological characteristics of the latter two species.

Most of the diagnoses and remarks on *Paracalanus* species were made based on a study of females. Despite the diagnostic characteristics of the swimming legs of females and males of *P. brasiliensis* sp. nov. being similar to those of some species of the genus, *P. brasiliensis* sp. nov. has unique characteristics that define it as a new species, namely the swimming legs seta and spine formula and ornamentation.

The original description of the *P. parvus* species complex provides insufficient diagnostic information regarding the morphology of the urosome and genital double somites. For example, for *P. serrulus*, *P. intermedius*, and *P. tropicus*, only figures of the species are available, whereas, for *P. quasimodo*, little information and few

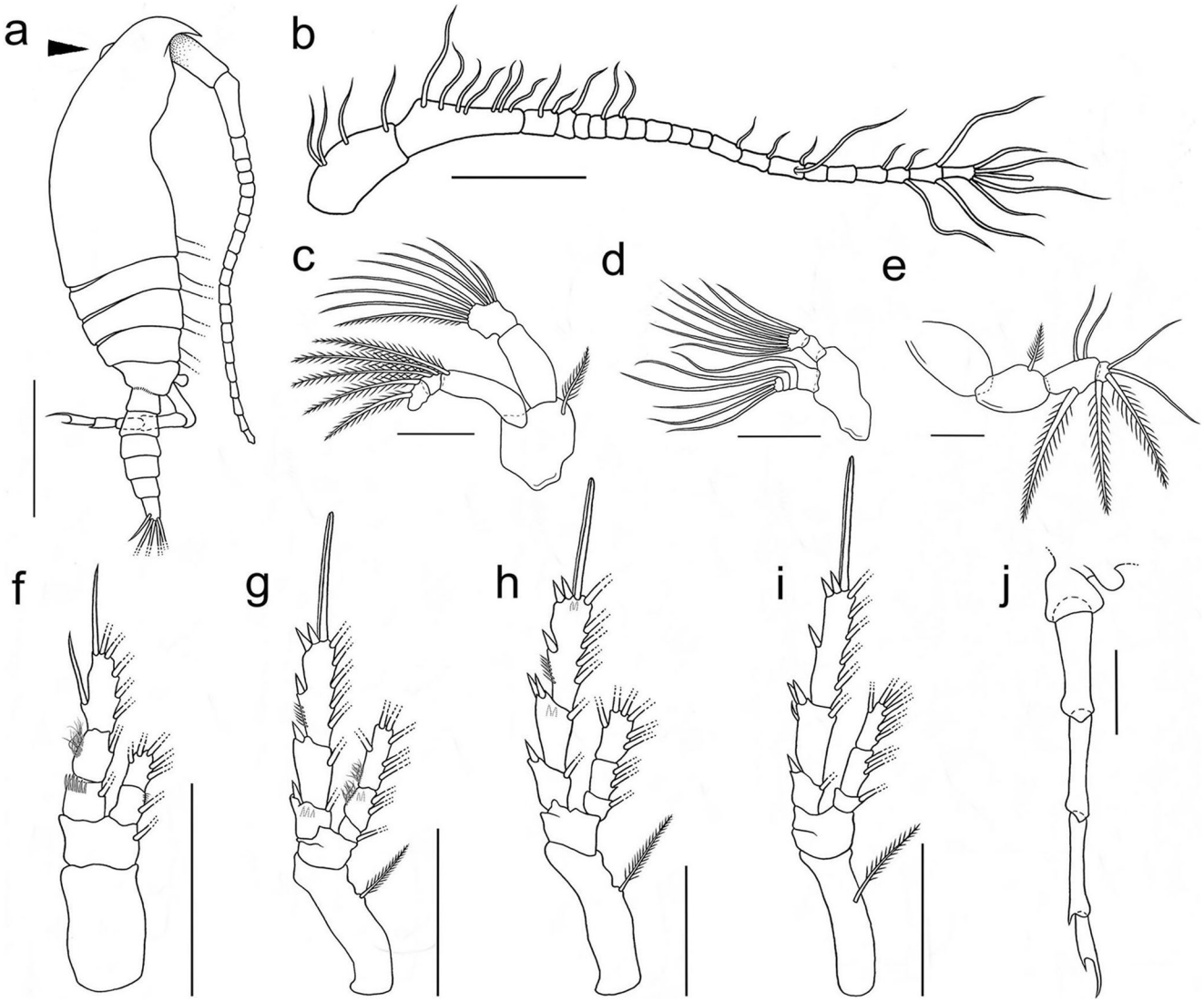

Fig. 16 Schematic drawings of the *Bestiolina brasiliensis* sp. nov. male. **a** Lateral view (allotype MNRJ-028871, paratypes DZUFRJ Copepoda-29095 and DZUFRJ Copepoda-45970), arrow indicating cephalic hump; **b** antennule (allotype MNRJ-028871, paratypes DZUFRJ Copepoda-29095 and DZUFRJ Copepoda-45970); **c** antenna (allotype MNRJ-028871, paratypes DZUFRJ Copepoda-29095 and DZUFRJ Copepoda-45970); **d** mandible (paratype DZUFRJ Copepoda-45970); **e** maxilliped (allotype MNRJ-028871, paratypes DZUFRJ Copepoda-29095 and DZUFRJ Copepoda-45970); **f** P1; **g** P2; **h** P3; **i** P4; **j** P5 (allotype MNRJ-028871, paratypes DZUFRJ Copepoda-29095 and DZUFRJ Copepoda-45970). Scale bars: a = 150 μm, b = 100 μm, c–e = 50 μm, f–i = 65 μm, j = 20 μm

figures are available. The material used herein is similar to that of *P. quasimodo*, *P. indicus*, and of the three groups of species of the *P. parvus* complex described by Hidaka et al. (2016) in terms of the presence of a genital double somite with denticles on the distal margin, even though the cluster of spinules above the spermatheca found in *P. quasimodo* (Bowman 1971) is not present. The specimens were also similar in the overall shape and arrangement of the genital field and seminal receptacles to the species of group 1 of the *P. parvus* complex (Hidaka et al. 2016); however, they had elliptical seminal receptacles rather than rectangular receptacles in the distal half. Hidaka et al. (2016) identified three species in the waters around Japan: *P. tropicus* (group 3), *P. indicus* (group 2), and an undescribed species (*Paracalanus* sp. (NWP)—group 1).

In relation to TL, *P. brasiliensis* sp. nov. was slightly longer than *P. nanus* (F 0.50–0.65, M 0.50–0.60) but smaller than the other species of the *P. parvus* complex (*P. indicus*: F 0.66–1.30, M 0.74–1.40; *P. parvus*: F 0.62–1.30, M 0.50–1.40; and *P. quasimodo*: F 0.75–1.00, M 0.82) found along the Brazilian coast, and *P. tropicus* (F 0.74–0.90), *P. intermedius* (F 0.88, M 0.78), and *P. serrulus* (F 1.02, M 0.97) (Razouls et al. 2005–2021).

Paracalanus nanus may be distinguished from other species by its small size, short antennules (barely reaching the end of the prosome), and the distal edges of exopodite 3 of non-

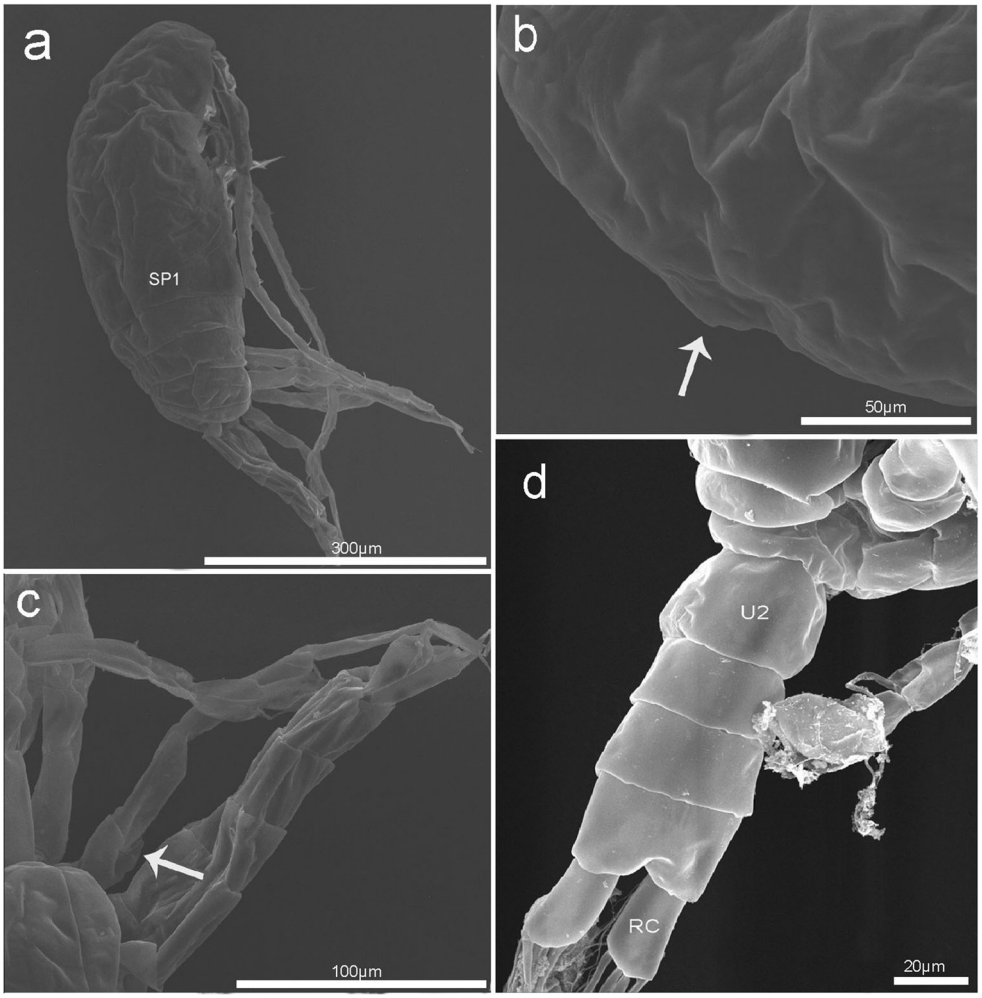

Fig. 17 *Bestiolina brasiliensis* sp. nov. male (paratype DZUFRJ Copepoda-29095). **a** Lateral view, showing the somite pedigerous 1 (SP1) fused to the cephalosome; **b** dorsal cephalic hump; **c** lateral view, urosome, and P5, arrow indicating rounded right lobe; **d** urosome: second urosomite (U2) and caudal rami (RC). Scanning electron micrograph (SEM)

serrated swimming legs 2–4 (Cornils and Held 2014; Fig. 1). *Paracalanus indicus*, *P. parvus*, and *P. quasimodo* are distinguished by differences in the serration of the distal outer edge of exopodite 3 from P2 to P4. *Paracalanus parvus* has a bulging forehead, while a dorsal bulge in the prosoma is present in *P. quasimodo* (Bowman 1971). Male *P. parvus* lacks a cephalic hump in the lateral view. *Paracalanus indicus* is characterized by the presence of posterior dorsal spines in the female genital double somite (Bradford 1978). According to Kasapidis et al. (2018), in their study of the taxonomic status and distribution of the *P. parvus* species complex in the Mediterranean and Black Seas, there are subtle morphological differences between *P. parvus*, *P. indicus*, and *P. quasimodo*, while the individual variability observed in Mediterranean specimens renders proper identification problematic.

There is a need to resolve the taxonomic ambiguities present and provide molecular databases with species data that have been validated by morphological and molecular taxonomy studies (Bucklin et al. 2016). Cornils and Held (2014) revealed 10–12 putative species in the *P. parvus* species complex, some of which may possibly be cryptic, with differing geographical distributions. In several instances, specimens that had been previously morphologically identified as a particular species were phylogenetically assigned to different species. In this study, *P. brasiliensis* sp. nov. sequences obtained from Brazil's central coast were compared with sequences from the lineages revealed by Cornils and Held (2014). The tree generated by the mtCOI gene fragments remained unchanged, and high bootstrap values were observed (ML 100%), indicating that the *P. brasiliensis* sp. nov. species found in the São João and Perequê-Açu estuaries

Table 3 Spine and setal formula of legs 1–4 in *Bestiolina brasiliensis* sp. nov.

Leg	Coxa	Basis	Exopodite			Endopodite		
			1	2	3	1	2	3
1	0-0	0-1	0-1	0-1	II,I,4	0-1	1,2,2	-
2	0-1	0-0	I-1	I-1	III,I,5	0-1	0-2	1,2,3
3	0-1	0-0	I-1	II-1	III,I,5	0-1	0-2	1,2,3
4	0-1	0-0	I-1	II-1	III,I,5	0-1	0-2	1,2,3

Table 4 Morphological comparison of species belonging to the *Paracalanus parvus* complex occurring on the Brazilian coast, based on the tables in Kang (1996) and Bradford (1978), and *Paracalanus nanus* schemes (Razouls et al. 2005–2021). *Personal observation

Taxonomic characters of the swimming legs	*P. quasimodo*	*P. indicus*	*P. parvus*	*P. nanus*	*P. brasiliensis* sp. nov.
P2-P4—coxopodite with spinules on the posterior surface	X	X	-	X	-
P2-P4—3rd serrated exopodite articulated	X	X (P4 little sawed)	X	X	X
P2—spinules between the spines of the 3rd articulated exopodite	X	X	-	X	-
P3—spinules between the spines of the 3rd articulated exopodite	X	X	-	X	-
P4—spinules between the spines of the 3rd articulated exopodite	X	-	-	-	-
P2-P4—spinules on the 2nd articulated endopodite	X	X	X	X	X
P3-P4—spinules on the 2nd articulated endopodite	X	X	Spinules row *	X	X

and specimens collected from the coastal waters of Argentina (*Paracalanus* sp. E. KF715983, *Paracalanus* sp. E. KF715986, and *Paracalanus* sp. E KF715987; Cornils and Held 2014) are co-specific. *Paracalanus brasiliensis* sp. nov. has morphological characteristics similar to those of *P. quasimodo*. These species are differentiated by the absence of spinules between the spines of the third articulated exopodite of legs P2–4 and bristles in the coxopodite in *Paracalanus brasiliensis* sp. nov. Genetic distance confirmed the separation of these species (Supplementary Material 1).

The large geographic gaps in the eastern Pacific, southwestern Atlantic, and Indian Oceans may indicate the existence of new species or cryptic species, which may alter the current biogeography of Paracalanidae. The present study describes a new *Paracalanus* species based on morphological and molecular evidence from the estuaries of southeastern Brazil and the waters of the coast of Argentina. The presence of *Paracalanus brasiliensis* sp. nov. was recorded in other places on the Rio de Janeiro coast, such as on Rasa Island (23° 03′ 38.10″ S and 43° 06′ 40.94″ O), Guanabara Bay in Niteroi (22° 55′ 24.29″ S and 43° 06′ 18.68″ O), and Arraial do Cabo (22° 58′ 14″ S–23° 01′ 04″ S and 42° 00′ 05″–42° 00′ 57″ W; Fig. 18). Therefore, it is necessary to review samples containing *P. brasiliensis* sp. nov. to identify potential locations where this species may occur.

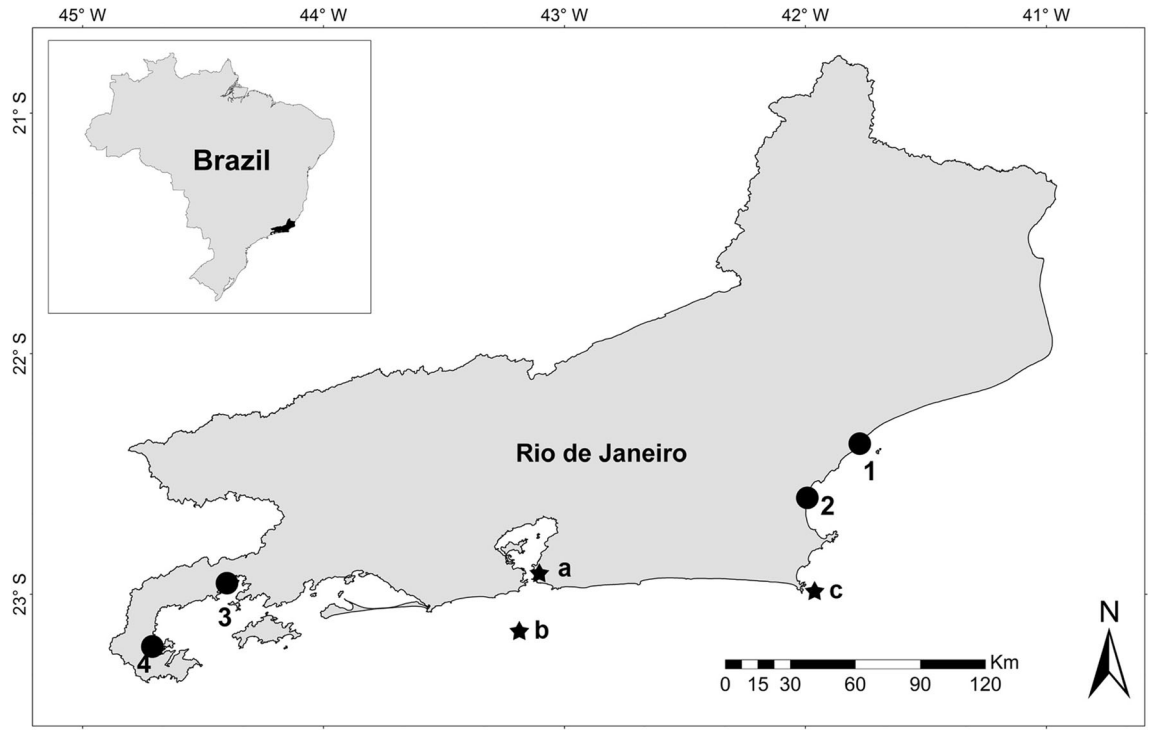

Fig. 18 Map of the sampled estuaries: 1, Macaé river estuary; 2, São João river; 3, Bracuí river; 4, Perequê-Açu river, and occurrence points of *Paracalanus brasiliensis* sp. nov. (a, Guanabara Bay; b, Rasa Island; c, Arraial do Cabo) in the Rio de Janeiro state, Brazil

Bestiolina brasiliensis sp. nov

The uniformity of the number of spinules and their location on the anterior face of the second exopodite of swimming legs 2–3 and the absence of spinules on the endopodite of swimming legs 3–4 seem to be sufficient to differentiate *Bestiolina brasiliensis* sp. nov. from all other *Bestiolina* species. According to Moon et al. (2010), the ornamentation of segment 2 of the exopodites of swimming legs 2–4 may play a fundamental role in the separation of similar species. Other characteristics also appear to be relevant, such as the presence of posterior spinules on swimming leg exopods 2–3 and the swimming leg endopodite, the absence of the small external spine on segment 1 of the exopodite of swimming leg 1, and the presence of a row of spinules on the posterior margin of the prosome (Suárez-Morales and Almeida-Artigas 2016; Table 5). The last two characteristics excluded the possibility of *Bestiolina brasiliensis* sp. nov. being *B. inermis*, *B. similis*, *B. zeylonica*, *B. amoyensis*, *B. arabica*, or *B. sarae* (Table 5).

Although the other species share similarities with the new species, *B. sinica* and *B. mexicana* do not possess spinules on swimming leg exopods 2–4 and 3–4, respectively. Although *B. mexicana* presents the posterior spinule formula on swimming leg 2 of 3,0,0, as does the new species, it is important to note that *B. brasiliensis* sp. nov. presented variation in the number of posterior spinules of this swimming leg (3, 0, 0 and 4, 0, 0). In turn, *B. coreana* does not have the same number or location of the spinules of swimming legs 2–4 and exhibits spicules of the form 4 + 3, 4 + 3, or 0 + 4 on endopodite 2 of swimming legs 2–4, respectively.

In *Bestiolina brasiliensis* sp. nov. females, a lack of the small spine on segment 1 of the swimming leg exopodite 1 and the presence of 12 spinules on the distal external margin on segment 1 of the same swimming leg were observed, a characteristic that has not been reported for any other species of this genus. However, the spinulation pattern on the exopodites' anterior and posterior faces and endopodites of swimming legs 2–4 are fundamental for differentiating one species from its congeners (Ali et al. 2007; Moon et al. 2010). The taxonomic key for females proposed by Moon et al. (2010) only allowed us to arrive at step 3. However, our specimens cannot be identified as either *B. zeylonica* or *B. sinica* due to the presence of spinules on the anterior-distal and posterior-distal faces of segments 1–3 of exopodites of P2–4. *Bestiolina brasiliensis* sp. nov. also has the smallest length, ranging from 0.39 to 0.60 mm (the measurements of the other species are shown in Table 5).

We described the seminal receptacle, although this structure is not used as a feature in the differentiation of *Bestiolina* species. It was not possible to compare the genital complex of *B. brasiliensis* females with that of the other species of *Bestiolina*, because it was not described in any of the nine species known worldwide.

Table 5 Morphological characters of the nine species of females of the genus *Bestiolina*. Data from Ali et al. (2007), Moon et al. (2010), Suárez-Morales and Almeyda-Artigas (2016), Dorado-Roncancio et al. (2019), and Razouls et al. (2005–2021), except for *Bestiolina brasiliensis* sp. nov. A, anterior face; P, posterior face

Taxonomic characters	Leg	*B. inermis*	*B. similis*	*B. sinica*	*B. zeylonica*	*B. amoyensis*	*B. arabica*	*B. coreana*	*B. mexicana*	*B. sarae*	*B. brasiliensis* sp. nov.
Body length (mm)	-	1.08	0.70–1.00	0.97–1.02	0.68–0.70	0.85–1.01	0.79–0.92	0.90–0.95	0.65–0.69	0.64–0.73	0.39–0.60
Cephalosome and first pedigerous somite	-	Separated	Fused	Fused	Fused	Fused	Fused	Fused	Separated	Fused	Separated
Posterior margin of rounded prosome with spine row	-	Absent	Absent	Present	Present	Present	Absent	Present	Present	Present	Present
External spine exopod segment 1	P1	Yes	Yes	No	Yes	Yes	Yes	No	No	Yes	No
Spinule number on posterior surface of segments 1–3 of the exopod	P2	0, 3, 0	0, 0, 3	Absent	3, 3, 2	2, 1, 1	Absent	0, 6, 3	3, 0, 0	Absent	A 0, 2, 0/3-4, 0, 0 P
	P3	?	0, 0, 3	Absent	0, 3, 2	1, 1, 2	Absent	0, 4, 0	Absent	Absent	A 0, 2, 0/0, 0, 2 P
	P4	?	Absent	Absent	Absent	1, 2, 1	Absent	0, 3, 0	Absent	Absent	A 0,2,0
Spinule number on anterior and posterior surfaces of segments 1–3 of the endopod 2	P2	4	0+5	4+4	4	5	3+0	P 4+3 P	2+4	3+4	0+2
	P3	?	0+5	5+4	4+3	4	3+0	P 4+3 P	2+0	3+4	Absent
	P4	?	Absent	0+4	0+ small spinules	0+ small spinules	Absent	P 0+4 P	3+0	Absent	Absent

A small number of males were found compared with females. These specimens were not in good preservation conditions, making it difficult to visualize the structures. Similar to other males of the genus, except for *B. amoyensis*, *Bestiolina brasiliensis* sp. nov. males present a cephalic hump. There were six spinules near the first external spine on the anterior face of the third segment of swimming leg exopodites 2–3 of the *Bestiolina brasiliensis* sp. nov. male. There have been no reports in the literature on this spinule pattern in other *Bestiolina* males.

Specimens belonging to the *Bestiolina* genus along the southeastern coast of Brazil were collected by Sterza and Fernandes (2006), Sterza et al. (2008), Pereira (2010, who identified *B. similis*), Araujo (2016), and Araujo et al. (2017b). The present work elucidates that the species referred to is *Bestiolina brasiliensis* sp. nov. Thus, a more detailed understanding of the morphological characteristics needed for identification is necessary to further clarify the records of *Bestiolina* in southeastern Brazil (Sterza and Fernandes 2006; Sterza et al. 2008; Pereira 2010).

Bestiolina brasiliensis sp. nov. can be distinguished from *B. similis* based on several morphological characteristics. The latter species has a long and thin rostrum, the presence of three spinules on the third segment of the P2–3 exopodites, five spinules on the second segment of the P2–3 endopodites, the absence of spinules on the posterior margin of the prosome, and the presence of the marginal spine on the first exopodite segment of P1. *Bestiolina brasiliensis* sp. nov. has a shortened and robust rostrum, the presence of two anterior spinules on the second segment of the P2–4 exopodite, 3–4 posterior spinules on the first segment, two spinules on the third segment of the P2–3 exopodite, two posterior spinules on the second segment of the P2 endopodite, the posterior margin of the prosome with a spinule row, and the absence of the marginal spine on the first segment of the P1 exopodite. This information has increased the list of known *Bestiolina* species to 10 and confirms its presence in the South Atlantic Ocean.

An analysis of the literature revealed a lack of molecular data for *Bestiolina* species. Molecular data based on the mtCOI gene are limited to only a few species of the *genus Bestiolina*, notably *B. similis*. The sequences of *Bestiolina brasiliensis* sp. nov. developed in the present study were analyzed using *Bestiolina* species in the GenBank database. An ML tree analysis determined that the sequences comprised a single clade, which was divergent from other *Bestiolina* species. Consequently, it may be concluded that our mtCOI sequences for *Bestiolina brasiliensis* sp. nov. represent the first molecular data for this species. In addition, it may be assumed that *B. similis* is either a species complex containing more than three cryptic species or that this situation is the result of misidentification [(*B. similis* in Kaneohe Bay, Hawaii, Jungbluth and Lenz 2013 and Cornils and Blanco-Bercial 2013; *B. similis* of Southwest Coast of India (unpublished); and *B. similis* of Palau, Mecherchar Island, Saitoh and Tamate (unpublished)].

Jungbluth and Lenz (2013) also observed significant genetic divergence (16%) between *B. similis* from Kaneohe Bay, Hawaii (intraspecific divergence of 0.2–1.0%) and *B. similis* from Palau, Micronesia, suggesting significant genetic isolation between species, which may be due to the more estuarine species of Kaneohe Bay inhabiting discontinuous environments that include a barrier reef separating estuarine and open-ocean specimens. In addition, differentiation within the *B. similis* clade itself was present based on individuals collected from Kaneohe Bay, and another cluster (intraspecific divergence of 0.2%) was formed, which was notably different from the primary clade (8.6–9.2%). Thus, the authors proposed a second cryptic *B. similis* species. Secondary clade specimens were found in the bay's northern and central regions, where the exchange of estuarine and coastal waters was greater than that of the southern region. In the same year, Cornils and Blanco-Bercial recovered the genus *Bestiolina* as a monophyletic clade but with moderate to low support (ML 69%; IB < 0.90).

The genus is commonly found in estuarine and coastal waters in tropical and subtropical regions. *Bestiolina* species are found at different temperatures and salinities, which are abiotic factors that directly influence copepod productivity. *Bestiolina similis* and *B. inermis* are distributed in the Pacific and Indian Oceans at salinities of 8–32 (Razouls et al. 2005–2021). Nonetheless, McKinnon et al. (2003) collected *B. similis* from the Haughton River, Australia, for cultivation under a controlled temperature (27 °C), and high densities of this copepod were observed in culture for 3 years. *Bestiolina arabica* was found near Bubiyan Island, in the Arabian Gulf, and the Indian Ocean and *B. zeylonica* has been found in Sri Lanka and the Indian Ocean at salinities and temperatures of 37 and 28.6 °C, respectively (Andronov 1972; Ali et al. 2007). *Bestiolina amoyensis* has been found in the Jiulong River in the China Sea, and *B. sinica* has been found in the China Sea estuaries, in waters with salinities ranging from 17.6 to 30.7 in 1966 and 1984, respectively. In Laguna de Mandinga in the Gulf of Mexico, *B. mexicana* has been found in waters with a salinity of 23.5 and temperature of 25 °C (Suárez-Morales and Almeyda-Artigas 2016). *Bestiolina coreana* inhabits brackish waters off the Yellow Sea coast and southwest Korean waters. However, Moon et al. (2010) reported the disappearance of *B. coreana* in the Younggwang region in North Korea when the temperature remained below 20 °C, and the salinities remained above 32. Finally, *B. sarae* has been found near Buenaventura in the Colombian Pacific, a region characterized by bays with temperatures of 26.6–29.7 °C and salinities of 1.3–30 (Dorado-Roncancio et al. 2019).

Bestiolina brasiliensis sp. nov. was abundant in estuarine waters with average temperatures of 24.5 ± 2.4 °C and salinities

ranging from 15 to 25 on the coast of Rio de Janeiro from March 2013 to March 2015. Except for the record of *B. mexicana* in the Gulf of Mexico (Suárez-Morales and Almeyda-Artigas 2016), no other species of *Bestiolina* have been previously recorded in the coastal waters of the Americas. The distribution pattern explained by Moon et al. (2010) may be behind the probable speciation of *Bestiolina*, with its origin in the Indo-Malaysian region. In addition, inter-oceanic dissemination that may have been due to Pliocene conditions that have been proposed for *Bestiolina* (Orsi and Ohtsuka 1999; Ohtsuka et al. 2018) may have contributed to the establishment of this genus in the different environments of its region of origin.

This study provides the first molecular database and morphological authentication of two new species of Paracalanidae off the central coast of Brazil in the southwestern Atlantic. Doubts regarding species identification highlight the importance of a detailed morphological description to obtain proper species-level descriptions, coupled with a phylogenetic analysis that is well supported by evolutionary models and reliable methods.

Supplementary Information The online version contains supplementary material available at https://doi.org/10.1007/s12526-021-01188-7.

Acknowledgements We thank our colleagues from the Laboratório Integrado de Zooplâncton e Ictioplâncton, Universidade Federal do Rio de Janeiro, especially Dra. Adriana Valente de Araujo, MSc Pedro F. de Carvalho, and Dr. Régis Vinícius Souza Santos who helped with the field work, Claudio de Souza Ressur for help with copepod sorting, and MSc Mariana Muget Julio for companionship during all stages of the manuscript. We would also like to acknowledge our colleagues MSc Victor Hugo Giordano Dias, MSc Isadora C. Toledo e Mello, and MSc Maria Clara da Costa Simas from the Laboratório de Metabolismo Macromolecular Firmino Torres de Castro, Universidade Federal do Rio de Janeiro, who helped with the molecular analysis. We thank Dra. Michelle Klautau for all the hours of explanation and suggestions in the analysis of phylogenetic trees. We thank MSc. Pedro Freitas de Carvalho for editing the micrographs, Dr. Luís Gustavo Barretto Rodrigues for the male drawings and Dr. Rafael Bendayan de Moura for the female drawings and for all the attention, availability, criticism, and suggestions. We would like to thank Editage (www.editage.com) for English language editing. We appreciate the reviewers' time to read critically our study and the many good suggestions provided that greatly improved the original MS.

Funding This study was funded by Fundação Carlos Chagas Filho de Amparo à Pesquisa do Estado do Rio de Janeiro (FAPERJ, E-26/110.363/2012).

Declarations

Conflict of interest The authors declare no competing interests.

Ethical approval This article does not contain any studies with animals performed by any of the authors.

Sampling and field studies All necessary permits for sampling and observational field studies have been obtained by the authors from the competent authorities and are mentioned in the acknowledgements when applicable.

Data availability All data generated and/or analyzed during the current study are included in this published article and its supplementary information files.

Author contribution SLCB designed and participated in the fieldwork study and revised the paper; COD and FGV-M analyzed the data and wrote the paper. AC analyzed the molecular data and revised the paper. RS designed the molecular analysis and revised the paper. All authors edited the manuscript.

References

Ali M, Al-Yaman F, Prusova I (2007) *Bestiolina arabica* sp. nov. (Copepoda, Calanoida, Paracalanidae), a new species from the northwestern Arabian Gulf. Crustaceana 80:195–205. https://doi.org/10.1163/156854007780121429

Altschul SF, Gish W, Miller W, Myers EW, Lipman DJ (1990) Basic Local Alignment Search Tool. J Mol Biol 215:403–410. https://doi.org/10.1016/S0022-2836(05)80360-2

Andronov VN (1970) Some problem of taxonomy of the family Paracalanidae (Copepoda). Zool Zh 49:980–985 [in Russian]

Andronov VN (1972) Veslonogie rachki *Bestiola* gen. n. (Copepoda, Paracalanidae). *Bestiola* gen. n. (Copepoda, Paracalanidae). Zool Zh 51:290–292 [in Russian]

Andronov VN (1977) *Paracalanus tropicus* sp. n. (Copepoda, Paracalanidae) iz yugovostochnoi Atlantiki. *Paracalanus tropicus* sp. n. (Copepoda, Paracalanidae) from south-east Atlantic. Zool Zh 56:154–156 [in Russian]

Andronov VN (1991) Ob izmenenii nazvanii nekotorykh taksonov Calanoida (Crustacea). Zool Zh 70:133–134 [in Russian]

Araujo AV (2016) Assembleias de Copepoda (Crustacea) em estuários do Rio de Janeiro: caracterização, impacto da poluição e relação com a teia trófica e o funcionamento do ecossistema. Ph.D. Thesis, Universidade Federal do Rio de Janeiro.

Araujo AV, Dias CO, Bonecker SLC (2017a) Effects of environmental and water quality parameters on the functioning of copepod assemblages in tropical estuaries. Estuar. Coast. Shelf Sci 194:150–161. https://doi.org/10.1016/j.ecss.2017.06.014

Araujo AV, Dias CO, Bonecker SLC (2017b) Differences in the structure of copepod assemblages in four tropical estuaries: importance of pollution and the estuary hydrodynamics. Mar Pollut Bull 115:412–420. https://doi.org/10.1016/j.marpolbul.2016.12.047

Bode M, Laakmann S, Kaiser P, Hagen W, Auel H, Cornils A (2017) Unravelling diversity of deep-sea copepods using integrated morphological and molecular techniques. J Plankton Res 39:600–617. https://doi.org/10.1093/plankt/fbx031

Boeck A (1865) Oversigt over de ved Norges Kyster jagttagne Copepoder henhorende til Calanidernes, Cyclopidernes og Harpactidernes Familier. Forh Vidensk-Selsk Kristiania 1864:226–282

Bowman TE (1971) The distribution of calanoid copepods off the southeastern United States between Cape Hatteras and southern Florida. Smithson Contrib Zool 96:1–58. https://doi.org/10.5479/si.00810282.96

Boxshall GA, Defaye D (2008) Global diversity of copepods (Crustacea: Copepoda) in freshwater. Hydrobiologia 595:195–207. https://doi.org/10.1007/s10750-007-9014-4

Bradford JM (1978) *Paracalanus indicus* Wolfenden and *Corycaeus aucklandicus* Kraemer, two neritic pelagic copepods from New Zealand. J R Soc NZ 8:133–141. https://doi.org/10.1080/03036758.1978.10429386

Bradford-Grieve JM (2008) *Mecynocera clausi* I.C. Thompson, 1888 (Copepoda: Calanoida) is a paracalanid. Zootaxa 1852:59–64. https://doi.org/10.11646/zootaxa.1852.1.5

Bradford-Grieve JM, Markhaseva EL, Rocha CEF, Abiahy B (1999) Copepoda. In: Boltovskoy D (ed) South Atlantic Zooplankton, Backhuys Publishers, vol 2. Leiden, Holanda, pp 869–1098

Bucklin A, Sundt R, Dahle G (1996) The population genetics of *Calanus finmarchicus* in the North Atlantic. Ophelia 44:29–45. https://doi.org/10.1080/00785326.1995.10429837

Bucklin A, Guarnieri M, Hil RS, Bentley AM, Kaartvedt S (1999) Taxonomic and systematic assessment of planktonic copepods using mitochondrial COI sequence variation and competitive species-specific PCR. In: Zehr JP, Voytek MA (eds) Molecular ecology of aquatic communities. Developments in hydrobiology, vol 138. Springer, Dordrecht, 401, pp 239–254. https://doi.org/10.1007/978-94-011-4201-4_18

Bucklin A, Lindeque P, Rodriguez-Ezpeleta N, Albaina A, Lehtiniemi M (2016) Metabarcoding of marine zooplankton: prospects, progress and pitfalls. J Plankton Res 38:393–400. https://doi.org/10.1093/plankt/fbw023

CHM – Centro de Hidrografia da Marinha (2016) Previsões de marés. Available at: https://www.marinha.mil.br/chm/tabuas-de-mare. Accessed 09 March 2021.

Claus C (1863) Die frei lebenden Copepoden mit besonderer Berucksichtigung der Fauna Deutschlands, der Nordsee und des Mittelmeeres. Verlag von Wilhelm Engelmann, Leipzig 1–230:1–37

COPPETEC - Coordenação de Projetos, Pesquisas e Estudos Tecnológicos (2014) Plano Estadual de Recursos Hídricos do Estado do Rio de Janeiro: Temas Técnicos Estratégicos - Fontes Alternativas para o Abastecimento do Estado do Rio de Janeiro, com Ênfase na RMRJ. Laboratório de Hidrologia e Estudos em Meio Ambiente. Rio de Janeiro, 2° Revisão. Available at: http://www.inea.rj.gov.br/cs/groups/public/documents/document/zwew/mdyy/~edisp/inea0062206.pdf. Accessed 09 March 2021.

Cornils A, Blanco-Bercial L (2013) Phylogeny of the Paracalanidae Giesbrecht, 1888 (Crustacea: Copepoda: Calanoida). Mol. Phylogenetics Evol 69:861–872. https://doi.org/10.1016/j.ympev.2013.06.018

Cornils A, Held C (2014) Evidence of cryptic and pseudocryptic speciation in the *Paracalanus parvus* species complex (Crustacea, Copepoda, Calanoida). Front Zool 11:1–19. https://doi.org/10.1186/1742-9994-11-19

Cronemberger FM (2014) Cartografia da dinâmica da paisagem no estado do Rio de Janeiro. Ph.D. Thesis. Universidade Federal Fluminense.

da Rosa JCL, Monteiro-Ribas WM, Fernandes LDA (2016) Herbivorous copepods with emphasis on dynamic *Paracalanus quasimodo* in an upwelling region. Braz j oceanogr 64:67–74. https://doi.org/10.1590/S1679-87592016105906401

Dahl F (1894) Die Copepoden fauna des unteren Amazonas. Ber naturf Ges Freiburg 8:10–23

Di Mauro R, Capitanio F, Viñas M (2009) Capture efficiency for small dominant mesozooplankters (Copepoda, Appendicularia) off Buenos Aires province (34°S–41°S), Argentina, using two plankton mesh sizes. Braz j oceanogr 57:205–214. https://doi.org/10.1590/S1679-87592009000300004

Dias CO, Bonecker SLC (2008) Inter-annual variability of planktonic copepods in a tropical bay in southeastern Brazil. Braz Arch Biol Techn 51:731–742. https://doi.org/10.1590/S1516-89132008000400011

Dorado-Roncancio J, Gaviria S, La Torre LB, Ahrens M (2019) A new species of *Bestiolina* (Crustacea, Copepoda, Calanoida, Paracalanidae) from coastal waters of the Colombian Pacific, including a worldwide key for the identification of the species. ZooKeys 846:1–18. https://doi.org/10.3897/zookeys.846.31497

Farias OG, Francisco CN, Senna MCA (2017) Avaliação de métodos de interpolação espaila aplicados à pluviosidade em região montanhosa no litoral Sul do estado do Rio de Janeiro. Rev Bras Climatol 21:172–185. https://doi.org/10.5380/abclima.v21i0.52065

Ferrari FD, Ivanenko VN (2008) Identity of the protopodal segments and ramus of maxilla 2 of copepods (Crustacea). Crustaceana 81:823–835. https://doi.org/10.1163/156854008784771702

Folmer O, Black M, Hoeh W, Lutz R, Vrijenhoek R (1994) DNA primers for amplification of mitochondrial cytochrome C oxidase subunit I from diverse metazoan invertebrates. Mol Mar Biol Biotech 3:294–299. Available at: https://pdfs.semanticscholar.org/943d/38b9d96f8222e883604822bcafb7930ca6da.pdf. Accessed 09 March 2021.

Francisco CN, Carvalho CN (2004) Disponibilidade hídrica - da visão global às pequenas bacias hidrográficas: o caso de Angra dos Reis, no Estado do Rio de Janeiro. Rev Geociênc 3:1–13. Available at: https://www.comiteguandu.org.br/downloads/ARTIGOS%20E%20OUTROS/Disponibilidade%20hidrica%20%20da%20visao%20global%20as%20pequenas%20bacias%20hidrograficas%20o%20caso%20de.pdf. Accessed 09 March 2021.

Francisco C, Oliveira C (2009) Sustentabilidade hídrica da Região Hidrográfica da Baía da Ilha Grande, RJ. Anais XIV Simpósio Brasileiro de Sensoriamento Remoto, pp. 4707–4714. Natal. Available at: http://marte.sid.inpe.br/col/dpi.inpe.br/sbsr%4080/2008/11.17.21.18.30/doc/4707-4714.pdf. Accessed 09 March 2021.

Giesbrecht W (1888) Elenco dei Copepodi pelagici raccolti dal Tenete di vascello Gaetano Chierchia durante il viaggio della R. Corvetta "Vettor Pisani" negli anni 1882-1885 e dal Tenente di vascello Francesco Orsini nel Mar Rosso, nel 1884. Atti Acad naz Lincei Rd Cl Sci fis mat nat 4(284–287):330–338

Giesbrecht W (1893) Systematik und Faunistik der pelagischen Copepoden des Golfes von Neapel und der angrenzenden Meeres-Abschnitte. Fauna u Flora Golf Neapel 19:1–831 pls.1–54

Goetze E (2003) Cryptic speciation on the high seas; global phylogenetics of the copepod family Eucalanidae. Proc R Soc B 270:2321–2331. https://doi.org/10.1098/rspb.2003.2505

Hidaka K, Itoh H, Hirai J, Tsuda A (2016) Occurrence of the *Paracalanus parvus* species complex in offshore waters south of Japan and their genetic and morphological identification to species. Plankton Benthos Res 11:131–143. https://doi.org/10.3800/pbr.11.131

Huys R, Boxshall GA (1991) Copepod evolution. The Ray Society, London

Jungbluth MJ, Lenz PH (2013) Copepod diversity in a subtropical bay based on a fragment of the mitochondrial COI gene. J Plankton Res 35:630–643. https://doi.org/10.1093/plankt/fbt015

Kang Y-S (1996) Redescription of *Paracalanus parvus* and *P. indicus* (Copepoda: Paracalanidae) recorded in the Korean waters. J Korean Fish Soc 29:409–413 [in Korean] http://www.koreascience.or.kr/article/JAKO199623607666051.pdf

Kasapidis P, Siokou I, Khelifi-Touhami M, Mazzoccihi MG, Matthaiaki M, Christou E, Puelles MLF, Gubanova A, Capua I, Batziakas S, Frangoulis C (2018) Revising the taxonomic status and distribution of the *Paracalanus parvus* species complex (Copepoda Calanoida) in the Mediterranean and Black Seas through as integrated analysis of morphology and molecular taxonomy. J Plankton Res 40:595–605. https://doi.org/10.1093/plankt/fby036

Kumar S, Stecher G, Tamura K (2016) Mega 7: Molecular Evolutionary Genetics Analysis Version 7.0 for bigger dataset. Mol Biol Evol 33:1870–1874. https://doi.org/10.1093/molbev/msw054%20

Laakmann S, Gerdts G, Erler R, Knebelsberger T, Martínez Arbizu P, Raupach MJ (2013) Comparison of molecular species identification for North Sea calanoid copepods (Crustacea) using proteome fingerprints and DNA sequences. Mol Ecol Resour 13:862–876. https://doi.org/10.1111/1755-0998.12139

Larkin MA, Blackshields G, Brown NP, Chenna R, Mcgettigan PA, Mcwillian H, Valentin F, Wallace LM, Wilm A, Lopez R, Thompson JD, Gibson TJ, Higgins DG (2007) Clustal W and Clustal X version 2.0. Bioinformatics 23:2947–2948. https://doi.org/10.1093/bioinformatics/btm404

Lee CE, Frost BW (2002) Morphological stasis in the *Eurytemora affinis* species complex (Copepoda: Temoridae). Hydrobiologia 480:111–128. https://doi.org/10.1023/A:102129320

Li SJ, Huang JQ (1984) On two new species of planktonic Copepoda from the estuary of Juilong River, Fujian, China. J Xiamen Univ 23: 381–390 [in Chinese]

Machida RJ, Miya MU, Nishida M, Nishida S (2004) Large-scale gene rearrangements in the mitochondrial genomes of two calanoid copepods *Eucalanus bungii* and *Neocalanus cristatus* (Crustacea), with notes on new versatile primers for the srRNA and COI genes. Gene 332:71–78. https://doi.org/10.1016/j.gene.2004.01.019

McKinnon AD, Duggan S, Nichols PD, Rimmer MA, Semmens G, Robino B (2003) The potential of tropical paracalanid copepods as live feeds in aquaculture. Aquaculture 223:89–106. https://doi.org/10.1016/S0044-8486(03)00161-3

McManus GB, Katz LA (2009) Molecular and morphological methods for identifying plankton: what makes a successful marriage? J Plankton Res 31:1119–1129. https://doi.org/10.1093/plankt/fbp061

Milne Edwards H (1840) Ordre des Copepodes. In: Histoire naturelle des Crustaces, comprenant l'anatomie, la physiologie et la classification de ces animaux. 3:411–529. Available at: https://www.biodiversitylibrary.org/page/16103940. Accessed 09 March 2021.

Moon SY, Lee W, Soh HY (2010) A new species of *Bestiolina* (Crustacea: Copepoda: Calanoida) from the Yellow Sea, with notes on the zoogeography of the genus. Proc Biol Soc Wash 123:32–46. https://doi.org/10.2988/09-12.1

Oakley TH, Wolfe JM, Lindgren AR, Zaharoff AK (2013) Phylotranscriptomics to bring the understudied into the fold: monophyletic Ostracoda, fossil placement, and pancrustacean phylogeny. Mol Biol Evol 30:215–233

Oda Y, Nakano S, Suh J-M, Oh H-J, Jin M-Y, Kim Y-J, Sakamoto M, Chang K-H (2018) Spatio temporal variability in a copepod community associated with fluctuations in salinity and trophic state in an artificial brackish reservoir at Saemangeum, South Korea. PLoS One 13:e0209403. https://doi.org/10.1371/journal.pone.0209403

Ohtsuka S, Shimono T, Hanyuda T, Shang X, Huang C, Soh HY, Kimmerer W, Kawai H, Ishimaru T, Tomikawa K (2018) Possible origins of planktonic copepods, *Pseudodiaptomus marinus* (Crustacea: Copepoda: Calanoida), introduced from East Asia to the San Francisco Estuary based on a molecular analysis. Aquatic Invasions 13(2):221–230. https://doi.org/10.3391/ai.2018.13.2.04

Orsi JJ, Ohtsuka S (1999) Introduction of the Asian copepods *Acartiella sinensis*, *Tortanus dextrilobatus* (Copepoda: Calanoida), and *Limnoithona tetraspina* (Copepoda: Cyclopoida) to the San Francisco Estuary, California, USA. Plankton Biol Ecol 46:128–131. Available at: http://www.plankton.jp/PBE/issue/vol46_2/vol46_2_128.pdf. Accessed 09 March 2021.

Pereira JB (2010) Composição, distribuição, biomassa e produção secundária do zooplâncton do sistema estuarino de Santos, São Paulo, Brasil. Ph.D. Thesis, Universidade de São Paulo. https://doi.org/10.11606/T.21.2011.tde-09082011-135919.

Razouls C, de Bovée F, Kouwenberg J, Desreumaux N (2005–2021) Diversity and geographic distribution of marine planktonic copepods. Sorbonne University, CNRS. Available at: http://copepodes.obs-banyuls.fr/en. Accessed 09 March 2021.

Salgado C, Peixoto M, Moura JD (2007) Caracterização espaço-temporal da chuva como subsídio à análise de episódios de enchentes no município de Angra dos Reis, RJ. Geosul 22:7–26. Available at: https://periodicos.ufsc.br/index.php/geosul/article/view/12607/11770. Accessed 09 March 2021.

Sars GO (1903) An account of the Crustacea of Norway, with short descriptions and figures of all the species: IV. Copepoda Calanoida. Bergens Museum, Bergen 171:pls.I–CII, suppl.I–VI. https://doi.org/10.5962/bhl.title.1164

Sars GO (1925) Copépodes particulièrement bathypélagique provenant des campagnes scientifiques du Prince Albert Ier de Monaco. Résult Camp scient Prince Albert I 69:pls.1–127.

Sewell RBS (1912) Notes on the surface-living Copepoda of the Bay of Bengal, I and II. Rec Indian Mus 7:313–382. https://doi.org/10.5962/bhl.part.28239

Sewell RBS (1914) Notes on the surface Copepoda of the Gulf of Mannar. Spolia zeylan 9:191–262. https://doi.org/10.5962/bhl.part.7319

Sewell RBS (1929) The Copepoda of Indian Seas, Calanoida. Mem Indian Mus 10:1–221. Available at: http://faunaofindia.nic.in/PDFVolumes/memoirs/010/01/0001-0407.pdf. Accessed 09 March 2021

Shen CJ, Bai SO (1956) The marine Copepoda from the spawning. Acta Zool Sin 8:177–234 (in Chinese, English summary)

Shen CJ, Lee FS (1963) The estuarine Copepoda of Chiekong and Zaikong Rivers, Kwangtung Province, China. Acta Zool Sin 15: 571–596 [in Chinese]

Shen CJ, Lee FS (1966) On the estuarine copepods of Chaikiang River, Kwangtung Province. Acta Zool Sin 3:213–223. Available at: http://en.cnki.com.cn/Article_en/CJFDTotal-DWFL196603005.htm. Accessed 09 March 2021

Silva Soares F, Nunes Francisco C, Nascimento de Carvalho C (2005) Análise dos fatores que influenciam a distribuição espacial da precipitação no litoral sul fluminense, RJ. Anais XII Simpósio Brasileiro de Sensoriamento Remoto. INPE, Goiânia, pp. 3365–3370. Available at: https://www.researchgate.net/publication/242565206_Analise_dos_fatores_que_influenciam_a_distribuicao_espacial_da_precipitacao_no_litoral_sul_fluminense_RJ. Accessed 09 March 2021.

Sterza JM, Fernandes LL (2006) Zooplankton community of the Vitória Bay estuarine system (Southeastern Brazil). Characterization during a three-year study. Braz J Oceanogr 54:95–105. https://doi.org/10.1590/S1679-87592006000200001

Sterza JM, Ovalle ARC, Fernandes LL (2008) Zooplankton distribution and abundance related to the hydrochemistry in a tropical bay (Southeast Brazil). Cah Biol Mar 49:229–245. https://doi.org/10.21411/CBM.A.82153B42

Suárez-Morales E, Almeyda-Artigas RJ (2016) A new species of *Bestiolina* (Copepoda: Calanoida: Paracalanidae) from the Northwestern Atlantic with comments on the distribution of the genus. Rev Mex Biodivers 87:301–310. https://doi.org/10.1016/j.rmb.2016.05.002

Tavaré S (1986). Some probabilistic and statistical problems on the analysis of DNA sequences. Lect Math Life Sci 17:57–86. Available at: http://www.damtp.cam.ac.uk/user/st321/CV_&_Publications_files/STpapers-pdf/T86.pdf. Accessed 09 March 2021.

Thompson IC (1888) Copepoda of Madeira and the Canary Islands, with description of new genera and species. J Linn Soc Zool 20:145–156. https://doi.org/10.1111/j.1096-3642.1888.tb01443.x

Walter TC, Boxshall G (2021) World of copepods database. Available at: http://www.marinespecies.org/copepoda. Accessed 09 March 2021

Wolfenden RN (1905) Notes on the collection of Copepoda. In: Stanley Gardiner J (ed) The Fauna and Geography of the Maldive and Laccadive Archipelagoes 2, suppl. 1:989–1040.